Slm1 and Slm2 are novel substrates of the calcineurin phosphatase required for heat stress-induced endocytosis of the yeast uracil permease.

Geert Bultynck, Victoria Heath, Alia Majeed, Jean-Marc Galan, Rosine Haguenauer-Tsapis, Martha Cyert

This manuscript has been accepted for publication in MOLECULAR AND CELLULAR BIOLOGY

Slm1 and Slm2 are novel substrates of the calcineurin phosphatase required for heat stress-induced endocytosis of the yeast uracil permease

Geert Bultynck*, Victoria L. Heath*‡, Alia P. Majeed*, Jean-Marc Galan+, Rosine Haguenauer-Tsapis+, and Martha S. Cyert*#

Running title: Calcineurin substrates required for Fur4 endocytosis

*Department of Biological Sciences, Stanford University, Stanford, California 94305-5020, USA.

+Institut Jacques Monod-CNRS, Universitie Paris VII, 2 place Jussieu, 75005 Paris, France

Corresponding author

Mailing address: Department of Biological Sciences, Stanford University, Stanford, California 94305-5020.

e-mail: mcyert@stanford.edu

Phone: (650)-723.9970

Fax: (650)-724.9945

‡ Present address: Institute for Biomedical Research, University of Birmingham, Edgbaston, Birmingham B15 2TT, UK

words in “Materials and Methods”: 2342

words in “Introduction, Results and Discussion”: 6679

ABSTRACT

The Ca^{2+}/calmodulin-dependent phosphatase, calcineurin, promotes yeast survival during environmental stress. We identified Slm1 and Slm2 as calcineurin substrates required for sphingolipid-dependent processes. Slm1 and Slm2 bind to calcineurin via docking sites that are required for their dephosphorylation by calcineurin, and are related to the PxIxIT motif identified in NF-AT. *In vivo*, calcineurin mediates prolonged dephosphorylation of Slm1 and Slm2 during heat stress, and this response can be mimicked by exogenous addition of the sphingoid base, phytosphingosine. Slm proteins also promote the growth of yeast cells in the presence of myriocin, an inhibitor of sphingolipid biosynthesis, and regulation of Slm proteins by calcineurin is required for their full activity under these conditions. During heat stress, sphingolipids signal turnover of the uracil permease, Fur4. In cells lacking Slm protein activity, stress induced endocytosis of Fur4 is blocked, and Fur4 accumulates at the cell surface in an ubiquitinated form. Furthermore, cells expressing a version of Slm2 that cannot be dephosphorylated by calcineurin display an increased rate of Fur4 turnover during heat stress. Thus, calcineurin may modulate sphingolipid-dependent events through regulation of Slm1 and Slm2. These findings, in combination with previous work identifying Slm1 and Slm2 as targets of Mss4/PIP2 and TORC2 signaling, suggest that Slm proteins integrate information from a variety of signaling pathways to coordinate the cellular response to heat stress.

INTRODUCTION

Calcineurin is a Ca^{2+}- and calmodulin-regulated serine/threonine protein phosphatase that is highly conserved from unicellular eukaryotes like the budding yeast, *Saccharomyces cerevisiae,* to humans and plays a critical role in Ca^{2+}-dependent signaling in these organisms (2). In mammalian cells, calcineurin mediates a plethora of physiological processes, including T-cell activation, skeletal and cardiac muscle development, long term potentiation and neural outgrowth, as well as pathophysiological processes, such as cardiac hypertrophy (7, 11, 28, 34). Specific inhibitors of calcineurin, FK506 and cyclosporin A, are in wide clinical use as immunosuppressants. In yeast cells, calcineurin is dispensable for growth under standard laboratory conditions. However, calcineurin activity becomes crucial for survival during specific stress conditions (15). Indeed, calcineurin is activated by a variety of environmental stresses, including high concentrations of Na^+, Li^+ and Mn^{2+} ions, high pH, heat stress, prolonged exposure to mating factor and in mutants with cell wall defects (reviewed in (15)). Calcineurin is a heterodimer consisting of a large catalytic (A) subunit (59 kDa), encoded in *S. cerevisiae* by two functionally redundant genes, *CNA1* and *CNA2,* and a small regulatory (B) subunit (19 kDa), encoded by *CNB1* (16, 17, 48, 53). Extracellular stresses promote a transient rise in the cytosolic Ca^{2+} concentration, and subsequent activation of calcineurin through binding of Ca^{2+}/calmodulin (reviewed in (15)). A major role of calcineurin is to regulate gene expression via the transcription factor Crz1, which, upon dephosphorylation by calcineurin, accumulates in the nucleus and directs the transcription of genes that promote cell survival during stress (56, 65, 66, 74).

An important feature of calcineurin signaling is its direct interaction with substrates and regulators via a conserved docking site that is distinct from sites of dephosphorylation. This property was first characterized for nuclear factor of activated T cells (NFAT), a family of mammalian transcription factors (1, 55). A small motif with the consensus amino acid sequence

"PxIxIT" is responsible for calcineurin binding to NFAT proteins and is required for their dephosphorylation (1). Furthermore, this docking site is conserved in other calcineurin-interacting proteins (18, 67). In yeast, calcineurin binds to Crz1 via the PxIxIT-related sequence, PIISIQ, and this site is required for its regulation by calcineurin (10).

We searched for novel calcineurin substrates by identifying calcineurin-interacting proteins. One of these proteins is Slm2, which was found to interact with the A-subunit of calcineurin in a genome-wide yeast two-hybrid screen (69). In this study, we show that Slm2 as well as its homologue, Slm1, bind calcineurin via a PxIxIT-related motif, and that both proteins are dephosphorylated by calcineurin *in vivo* and *in vitro.* In each case, this dephosphorylation requires the calcineurin-docking site.

Recent studies provide insights into the physiological functions of Slm1 and Slm2 (4, 27). *SLM1* and *SLM2* form an essential gene pair, and each gene product contains a conserved Pleckstrin Homology domain (PH domain) that binds phosphatidyl inositol 4,5-bisphosphate (PIP_2) (75). The essential lipid kinase, Mss4, synthesizes PIP_2 in the plasma membrane (19, 40), and this PIP_2 production recruits Slm1 and Slm2 to the cell periphery (75). Slm proteins seem to be critical downstream effectors of Mss4/PIP_2, as *slm1Δ* is synthetically lethal with *mss4*^{ts}, and like Mss4, Slm1 and Slm2 are required for polarization of the actin cytoskeleton (4, 27). In addition, Slm1 is phosphorylated by TORC2, a Tor2 kinase-containing complex that regulates actin cytoskeleton organization; and this phosphorylation is required for its localization to the cell periphery (4). Furthermore, an *avo3*^{ts} mutant, which lacks an essential subunit of the TORC2 complex, is suppressed by *SLM1* overexpression (39). Thus, Slm proteins are downstream effectors of both PIP_2 and TORC2 signaling.

In addition, Slm proteins participate in the cellular response to heat stress. Heat stress causes a transient increase in PIP_2 levels as well as a transient depolarization of the actin cytoskeleton (19). The temporal pattern of Slm1 phosphorylation is modulated in response to

heat stress and parallels the depolarization/repolarization of the cytoskeleton (4). Furthermore, *slm1*^{ts} *slm2Δ* cells are suppressed by mutations that activate the cell integrity pathway, a key component of cell tolerance to elevated temperature (4, 50). In this study we show that high temperature leads to increased phosphorylation of Slm1 and Slm2 by protein kinases, which is counteracted by their dephosphorylation by calcineurin.

Another component of the heat stress response is the production of sphingolipids. When cells are exposed to high temperature, levels of dihydrosphingosine and phytosphingosine, the major sphingoid bases in yeast, increase within minutes, and are required for tolerance to heat stress (21, 44). One consequence of phytosphingosine accumulation is inhibition of nutrient uptake via turnover of permeases, such as the uracil permease Fur4 (13, 14, 30). Recently, the PDK1-related kinases, Pkh1 and Pkh2 were identified as signaling effectors of phytosphingosine (12, 29, 77). These kinases are required to maintain cell integrity and for endocytosis and act in part through activation of downstream kinases including Pkc1, Ypk1 and Ypk2 (29, 41, 61). Interestingly, overexpression of *YPK1* confers resistance to myriocin, a potent inhibitor of the *de novo* sphingolipid biosynthesis pathway (68).

Here, we demonstrate a novel role for Slm1 and Slm2 in sphingolipid signaling and/or metabolism. We show that the Slm proteins are required for growth of yeast cells in the presence of myriocin and for endocytosis of Fur4 during heat stress. Both of these aspects of Slm function are altered by mutations that abrogate the ability of calcineurin to dephosphorylate Slms, suggesting that calcineurin acts through Slm1 and Slm2 to regulate sphingolipid-dependent events. Thus, Slm1 and Slm2 apparently coordinate TORC2, Mss4/PIP_2, sphingolipid and Ca^{2+}/calcineurin signaling to drive actin polarization and promote endocytosis of a nutrient permease during heat stress.

Materials and Methods

Yeast strains and media. Yeast media and culture conditions were essentially as previously described (62) except that twice the level of amino acids and nucleotides was used in synthetic media. Yeast transformations were performed with the lithium acetate method (5). Yeast strains are listed in Table1; strains from the yeast deletion collection were purchased from Open Biosystems (Huntsville, AL).

VHY61 is a haploid segregant of BY4743, *slm2Δ:::KAN*^{R} (deletion collection). To create GBY59, the *SLM1* open reading frame of VHY61 transformed with pRS316-*SLM2* was replaced by the natMX4 cassette via PCR, using pAG25 as template (32). This strain was then transformed with all other Slm alleles expressed from different plasmids. The pRS316-Slm2 plasmid was lost by streaking out the transformants on selective medium supplemented with 5-fluorootic acid (5FOA; U.S. Biochemicals, Swampscott, MA).

The plasmids used in this study are reported in Table 2. Recombinant DNA procedures were performed as previously described (5). All genes were initially cloned by amplification of genomic DNA with Vent polymerase or with Taq High Fidelity polymerase (Invitrogen, Beverly, MA) to create fragments flanked by restriction sites. Cloned genes were subcloned in different expression vectors by PCR amplification of plasmid DNA with PfuUltra HotStart polymerase (Stratagene, Cedar Creek, TX). All clones were sequenced by Sequetech Corporation (Mountain View, CA).

For yeast-two hybrid studies, the pGBT9 and pACT2 vectors were used to create GAL4 binding and activation domain fusions, respectively. All full-size and truncated versions of *SLM1* and *SLM2* were cloned as *Nco*I/*Xho*I fragments into pACT2 and as *Xma*I/*Sal*I fragments into pGBT9. A PCR-based deletion strategy was used to delete amino acids 639 to 644 of *SLM2*, encoding PEFYIE and to delete amino acids 672 to 677 of *SLM1*, encoding PNIYIQ. All GST-

and GFP-expression plasmids were constructed by cloning *SLM1* and *SLM2* as *Xma*I/*Xho*I fragments. For pRS316 and pRS313 plasmids, we first cloned the promoter of *SLM1* and *SLM2* (500 bp upstream sequence of the ORF, respectively) as *Spe*I/*Xma*I fragments. We then cloned the different *SLM* alleles as *Xma*I/*Xho*I fragments. *FUR4* was subcloned in the pVT102-U overexpression plasmid as a *Xba*I/*Xho*I fragment amplified by PCR using pfF as template (70).

Chemical compounds. Myriocin (Sigma, St. Louis, MO) was dissolved in methanol at a stock concentration of 1 mg/ml and was stored at 4 ºC. Aureobasidin A (Takara Mirus Bio, Madison, WI) was dissolved in ethanol at a stock concentration of 1 mg/ml and was stored at 4 ºC. Phytosphingosine (Sigma) was dissolved in ethanol at a stock concentration of 20 mM and was stored at -20 ºC. All these stock solutions were put at room temperature 30 min prior to their addition to media. FK506 (LC Laboratories, Woburn, MA) was dissolved in a mixture of 90% ethanol and 10% Tween-20 at a stock concentration of 20 mg/ml and stored at 4 ºC. FK506 was used at a final concentration of 2 μg/ml.

Spot assays. Growth of various strains was assessed by spotting serial dilutions of stationary-phase yeast cultures on YPD plates containing various drugs or selective medium (for yeast two-hybrid analysis). Cultures were diluted to an OD_{600} of 2.0, and five to six five-fold serial dilutions were prepared and transferred to the plates. Plates were incubated at 30 ºC for 2 to 3 days, unless otherwise indicated.

Yeast two-hybrid analysis. Yeast-two hybrid assays were performed by introducing combinations of Gal4p activation and binding domain fusions into strain PJ69-4A, which contains a GAL1 promoter-*HIS3* reporter gene, a GAL2 promoter-*ADE2* reporter gene and a GAL7 promoter-lacZ reporter gene (42, 43). Strains were grown in selective medium and spotted onto synthetic medium containing and lacking either histidine or adenine. β-

galactosidase activity was determined in exponentially growing yeast cells at 30 °C as follows: Cells were harvested and washed once, and the cell pellets were frozen. Cells were broken using glass bead lysis in Breaking Buffer (100 mM Tris at pH 8, 20% glycerol, 1 mM DTT) plus protease inhibitors (1 mM PMSF, 1 mM benzamidine, 2 μg/mL leupeptin, 2 μg/mL aprotinin). β-Galactosidase activity was measured at 30 °C in a microtiter plate using 10 μl of total protein extract, 90 μL of Z-buffer (100 mM Na_2HPO_4, 40 mM NaH_2PO_4, 10 mM KCl, 1 mM $MgSO_4$, 0.027% β-mercaptoethanol), and 20 μL of 4 mg/mL ONPG (*O*-nitrophenyl-β-D-galactopyranoside, Sigma). Protein concentrations of all cell extracts were determined using the Bio-Rad protein assay (Bio-Rad, Richmond, CA) and were used to calculate the specific β-galactosidase activity. Values result from the average of two independent extracts each measured in triplicate.

Isolation of GST-tagged proteins. Yeast cells expressing GST-Slm1 or GST-Slm2 were grown at 30 ºC in synthetic medium lacking uracil with 4% raffinose as carbon source. Cells were diluted to an OD_{600} of 0.2 in synthetic medium lacking uracil with 4% raffinose as carbon source. After 4 hours, expression of the GST-fusion proteins was induced by the addition of 2% galactose for 4 hours. 2 μg/ml FK506 was added 30 minutes prior to the addition of galactose as noted. Cells were harvested by centrifugation and cell pellets were frozen at -80 ºC prior to preparation of extracts. Cells were broken by using glass bead lysis in Modified RIPA buffer (20 mM Tris-HCl [pH 7.4], 2 mM EDTA, 750 mM NaCl, 1% Triton X-100, 1 mM DTT), supplemented with protease inhibitors (1 mM PMSF, 1 mM benzamidine, 1 μg/ml pepstatin A, 1 μg/ml leupeptin, 1 μg/ml aprotinin) and phosphatase inhibitors (5 mM sodium phosphate, 10 mM sodium molybdate, 20 mM sodium fluoride, 10 mM sodium pyrophosphate, 5 mM EGTA, and 5 mM EDTA). Protein concentrations of all cell extracts were determined using the Bio-Rad protein assay. Protein extracts (150 to 350 μg) were diluted 5-fold in Dilution Buffer (20 mM Tris-HCl

[pH 7.4], 2 mM EDTA, 150 mM NaCl, 1 mM DTT, 1 mM PMSF, 1 mM benzamidine, 1 μg/ml pepstatin A, 1 μg/mL leupeptin, 1 μg/mL aprotinin) and incubated for 2 hours with glutathione-sepharose beads pre-equilibrated with Dilution Buffer at 4 ºC. Beads were washed three times in Wash Buffer (20 mM Tris-HCl [pH 7.4], 2 mM EDTA, 150 mM NaCl, 0.5% Triton X-100, 1 mM DTT, 1 mM PMSF, 1 mM benzamidine, 1 μg/ml pepstatin A, 1 μg/mL leupeptin, 1 μg/mL aprotinin). GST-fusion proteins were eluted in SDS sample buffer, separated on a 6.75% SDS-PAGE and transferred to a nitrocellulose membrane. Blots were incubated either with the rabbit polyclonal anti-phosphorylated proteins (Pan) antibody (Zymed Laboratories Inc., South San Francisco, CA; diluted 1/250) or the mouse 4C10 monoclonal anti-GST (Covance/Berkeley Antibody Co., Richmond, CA; diluted 1/1000) and then with horseradish peroxidase-conjugated anti-rabbit or anti-mouse immunoglobulin (Amersham, Arlington Hts, IL).

Detection and quantification of immunoreactive bands by immunoblotting. Immunoreactive bands on western blots were visualized with an ECL kit (Pierce, Rockford, IL) and subsequent exposure to Biomax MR film (VWR, San Francisco, CA). For each blot, multiple exposures were taken, ranging from 6 seconds to several minutes. Each exposure was scanned to obtain a digital image, and immunoreactive bands were quantified using ImageJ (version1.34n) software (http://rsb.info.nih.gov/ij/). Data presented in the figures, represents analysis of a single optimal exposure for each blot. This optimal exposure was determined empirically; an exposure for which the signal from the most intense band was ≤ 30% of its observed maximum was used, thus ensuring that quantification was not distorted by signal saturation. In each case 2 to 4 independent experiments were conducted; the data displayed in the figure depicts results from a single representative experiment.

***In vitro* phosphatase assay.** DD12 cells expressing GST-Slm1 or GST-Slm2 were grown for 4 hours in synthetic medium lacking uracil and methionine with 4% raffinose as carbon.

Expression of the GST-fusion proteins was induced by the addition of 2% galactose. Lysis of the cells and purification of the GST-fusion proteins were performed as described above. GST-fusion proteins bound to the glutathione-Sepharose 4B beads were washed twice in Wash Buffer containing protease inhibitors and phosphatase inhibitors, twice in Wash Buffer containing protease inhibitors only, and twice in CP buffer (50 mM Tris-HCl [pH 7.5], 1 mM $MgCl_2$, 1 mM DTT) containing protease inhibitors. Washed beads were divided among four tubes prior to different phosphatase treatments. Phosphatase assays were performed in a total of 100 µl in CP buffer for calcineurin and in the supplied buffer for λ-phosphatase (New England Biolabs, Beverly, MA); 500 U of recombinant human calcineurin (Calbiochem, San Diego, CA), 2600 U of calmodulin (Calbiochem), or 10 µl of λ-phosphatase (New England Biolabs) was used per assay. Where indicated, $CaCl_2$ was added to a final concentration of 40 mM and EGTA to 10 mM. Phosphatase assays were incubated at 30 °C for 30 min; the supernatant was then removed, and SDS-PAGE sample buffer was added to the beads. Samples were analysed by SDS-PAGE (7.5% gels) and blotted as described above. Immunoreactive bands were visualized as described above

Fluorescence microscopy. The localization of GFP-Slm2, GFP-Slm2$^{\Delta PEFYIE}$, GFP-Slm1 and GFP-Slm1$^{\Delta PNIYIQ}$ was examined in strains GBY104 – GBY107. Liquid cultures were set up in synthetic medium lacking histidine and supplemented with methionine (75 mg/liter). Log-phase cultures, OD_{600} of 1.0, were concentrated by brief centrifugation and mounted on microscope slides. Cells expressing a single GFP fusion were visualized with a Nikon Eclipse E600 microscope with fluorescence optics and an HB100 mercury lamp. Fluorescein filter sets (Chroma Technology Co., Brattleboro, VT) were used to visualize GFP. Photos were taken with a Hammamatsu digital charge-coupled device 47420-95 camera and QED software (QED Imaging). Actin cytoskeleton staining was performed on cells grown to log phase. Cells were then fixed for 30 min at room temperature by the direct addition of 37% formaldehyde stock to a

final concentration of 5%. Fixed cells were collected, washed twice with PBS supplemented with 1 mg/ml BSA. Then, 0.04 U/μl of Texas red-X phalloidin (Molecular Probes, Eugene, OR) was added for 30 min at room temperature to stain actin. Cells were washed three times with PBS supplemented with 1 mg/ml BSA. Cells were resuspended in mounting medium and cells were visualized as described above, except for the use of a rhodamine filter. Only cells in which the bud was significantly smaller than the mother cell were analyzed.

Fur4 turnover. Wild-type cells and *slm1*^{ts} *slm2Δ* cells transformed with pVT102u-Fur4 (pGB047) were grown at 25 ºC in selective synthetic medium lacking uracil to log phase. Cells were shifted to 40 ºC, OD_{600} was measured before the shift, and at the indicated time points 3 OD_{600} units of yeast cells (i.e. 3 mls of culture at OD600 of 1.0 or the equivalent) were removed. Cells were harvested and resuspended in H_2O, yielding a total volume of 500 μl. Cells were lysed for 10 minutes on ice by adding 50 μl 1.85 M NaOH supplemented with 300 mM β-mercaptoethanol. Proteins were precipitated on ice for 10 minutes by adding 50 μl of 50% trichloroacetic acid (TCA). Proteins were collected by centrifugation and the protein pellets were dissolved in 120 μl urea/SDS sample buffer (8 M urea, 5% SDS, 200 mM Tris-HCl [pH 6.8], 0.1 mM EDTA pH 8, 0.1% bromophenol blue, 100 mM DTT) supplemented with 100 mM Tris. Samples were heated for 10 min at 37 ºC just before loading on a 4-15% SDS-PAGE (Bio-Rad, Richmond, CA). After Western blotting to nitrocellulose, membranes were incubated with the rabbit polyclonal anti-Fur4 (1/15000 dilution) and with the mouse monoclonal 22C5 anti-Pgk1p (1/5500 dilution; Molecular Probes). After image analysis, the anti-Fur4 signal was corrected for the Pgk1p loading control and all values were normalized to the 0 min time point. A similar approach was taken for determining the Fur4 turnover rate in cells expressing GST-Slm2, GST-Slm2$^{\Delta PEFYIE}$, GST-Slm1 or GST-Slm1$^{\Delta PNIYIQ}$, except that pfF was used for the overexpression of Fur4.

Uracil uptake assay. Exponentially growing wild-type or *slm1*^{ts} *slm2Δ* cells transformed with pVT102u-Fur4 (pGB047) and grown in selective synthetic medium lacking uracil at 25 °C were preshifted 10 min at 40 ºC. At time zero, cells were treated with cycloheximide (CHX) (10 μg/ml). The uracil uptake was measured as previously described (31). Yeast culture (1 ml) were incubated with 5 μM [^{14}C]uracil (Amersham, Arlington Hts, IL) for 20 s at 30 °C and quickly filtered through Whatman GF/C filters. Filters were washed twice with ice-cold water and then counted for radioactivity.

Membrane preparation for detection of ubiquitinated Fur4. Exponentially growing yeast cells transformed with pVT102u-Fur4 (pGB047) and grown in selective synthetic medium lacking uracil at 25 °C were shifted to 40 ºC. Ten minutes after heat shock, cycloheximide (100 μg/ml) was added for 50 min. Yeast cells (8.5 OD_{600} units) were harvested before (0 min) and after (60 min) the temperature shift by centrifugation in the presence of 10 mM sodium azide, washed once in distilled water plus 10 mM sodium azide, and used to prepare membrane-enriched fractions, as described in (23). Washed cells were transferred to a conical 1.5-ml Eppendorf tube and suspended in 150 μl of lysis buffer (100 mM Tris-HCl [pH 7.4], 150 mM NaCl, 5 mM EDTA plus protease inhibitors and 25 mM freshly prepared *N*-ethylmaleimide to prevent artifactual deubiquitination). All subsequent steps were carried out at 4 °C. Chilled glass beads (150 μl) were added, and the cells were lysed by vigorous vortex mixing for 7 times for 1 min each, separated by 1 min intervals. The homogenate was collected and centrifuged at 3,000 rpm for 2 min to remove unbroken cells and debris. The total protein extract was centrifuged for 45 min at 16100 x g. This pellet was washed by suspension in 100 ml lysis buffer supplemented with 5 M urea, incubated for 30 min on ice and centrifuged for 45 min at 16100 x g. The resulting pellet was suspended in 100 μl of lysis buffer and TCA was added to 10% to precipitate proteins and to prevent proteolysis by residual endogenous proteases. Protein precipitates were collected by sedimentation (16100 x g, 45 min). The protein precipitates were

suspended in 40 μl urea/SDS sample buffer supplemented with 100 mM Tris and 8 ul of this mixture was analyzed on a 4-15% SDS-PAGE (Bio-Rad, Richmond, CA). After Western blotting, membranes were incubated with anti-Fur4, developed, stripped with Restore™ Western Blot Stripping Solution (Pierce, Rockford, IL) and reprobed with anti-ubiquitin (P4D1 monoclonal, Santa Cruz Biotechnology, Santa Cruz, CA).

RESULTS

Slm1 and Slm2 interact with and are physiological substrates of calcineurin.

Genome-wide yeast two-hybrid analyses demonstrated an interaction between the A subunit of calcineurin and the ORF *YNL047C*, characterized as *SLM2*. We used yeast two-hybrid assays to confirm this observation and to investigate whether the A subunit of calcineurin was also able to interact with Slm1, which is 53% identical to Slm2 at the protein level. Cna1 and Cna2 were fused in frame with the Gal4 DNA-binding domain, whereas Slm1 and Slm2 were fused in frame with the Gal4 activation domain. Combinations of these constructs were expressed in strain PJ69-4A, containing three different reporter genes, each driven by a different promoter. The *GAL1* promoter-*HIS3* reporter is activated by low- and high-affinity interactions, whereas the more stringent *GAL2* promoter-*ADE2* reporter and *GAL7*-lacZ reporter are only activated by high-affinity interactions. As indicated in Fig.1A, both Slm1 and Slm2 interacted with Cna1 as well as Cna2 and allowed growth of strains on medium lacking histidine. However, only Slm2 was able to activate the *ADE2* and LacZ reporter genes, suggesting that Slm2 interacts with Cna1 and Cna2 with higher affinity than Slm1. We believe these differences in reporter activation reflect differences in affinity, since the Slm1- and Slm2- Gal4 activation domain fusion proteins are expressed at similar levels and show identical interactions in two hybrid assays with other gene products, such as Avo2, a subunit of the TORC2 protein kinase complex (data not shown).

Since Slm1 and Slm2 interacted with both calcineurin A subunits, we determined whether they were substrates of calcineurin *in vivo* (Fig.1B). Functional N-terminal GST fusions of Slm1 and Slm2 were expressed in wild type and calcineurin-null cells (*cnb1Δ*, lacking the calcineurin regulatory B subunit). After purification of GST-Slm1 and GST-Slm2 on Glutathione-Sepharose 4B beads, we examined their electrophoretic mobility by Western blotting with anti-

GST antibodies. In addition, we determined the extent of phosphorylation of Slm1 and Slm2 by Western blotting with a mixture of antibodies that recognizes phosphorylated serine, threonine and tyrosine residues (see Materials and Methods). We will refer to this as the phospho-antibody. As shown in Fig. 1B, Slm2 displayed a calcineurin-dependent change in phosphorylation, as is evident from the shift in electrophoretic mobility (anti-GST blot) and from the dramatic difference in extent of phosphorylation (anti-phospho blot) in extracts of wild type cells versus *cnb1Δ* cells. Slm1 also showed a calcineurin-dependent change in electrophoretic mobility and in the extent of phosphorylation, however, the differences were more subtle. Quantification of the signal obtained with the phospho-antibody showed a ~20 - 30% increase in the phosphorylation of GST-Slm1 in cells lacking calcineurin activity that was consistently and reproducibly observed. As we will show (Fig. 3) the dephosphorylation of Slm1 by calcineurin becomes more evident under specific stress conditions (such as heat stress), leading to hyperphosphorylation of GST-Slm1 when calcineurin function is compromised. These data indicate that both Slm1 and Slm2 display calcineurin-dependent changes in phosphorylation *in vivo*.

We then used an *in vitro* dephosphorylation assay to show that Slm1 and Slm2 are direct substrates of calcineurin. GST-Slm1 and GST-Slm2, purified from calcineurin-deficient cells, showed an increased mobility and reduced extent of phosphorylation when incubated with purified Ca^{2+}/CaM-activated calcineurin (Fig. 1C). These changes were abolished by inhibiting calcineurin with EGTA, a Ca^{2+} chelator (Fig. 1C). Calcineurin was able to perform a robust dephosphorylation of GST-Slm2 (> 80% reduction in phosphorylation in comparison to untreated GST-Slm2), and had a partial effect on the phosphorylation state of GST-Slm1 (~30% reduction in phosphorylation in comparison to untreated GST-Slm1). In agreement with these changes in the extent of phosphorylation, the protein samples incubated with active purified calcineurin showed increased electrophoretic mobility (anti-GST blot). As a control, both proteins were completely dephosphorylated by λ-phosphatase treatment.

Hence, both Slm1 and Slm2 are calcineurin substrates. However, both the *in vivo* and *in vitro* experiments show that while the majority of Slm2 phosphorylation is subject to dephosphorylation by calcineurin, only a portion of the phosphorylated sites of Slm1 are dephosphorylated by calcineurin.

Calcineurin binds to a conserved C-terminal PxIxIT-related motif in Slm1 and Slm2.

To further examine the physiological relevance of the calcineurin-dependent dephosphorylation of Slm1 and Slm2, we mapped the calcineurin-binding site in Slm1 and Slm2. A series of N-terminal deletion constructs of Slm1 and Slm2 were tested for interaction with Cna1 using the yeast 2-hybrid method (Fig. 2A). All N-terminally truncated proteins interacted with calcineurin, suggesting that the calcineurin-docking site was located in the C-terminal protein of Slm1 and Slm2. Many proteins interact with calcineurin via a docking motif with a consensus "PxIxIT" sequence. We found a potential PxIxIT-related motif in the C-terminal tail of Slm2 (PEFYIE) that was similar in Slm1 (PNIYIQ) (Fig. 2B). Slm1 and Slm2 lacking their C-terminal tails (aa 1-672 and aa 1-639, respectively) failed to interact with Cna1 as did mutant constructs in which just the PxIxIT motif was deleted (Slm1, aa 1-686$^{\Delta PNIYIQ}$ and Slm2, aa 1-657$^{\Delta PEFYIE}$) (Fig. 2A). Similar results were obtained for interactions with Cna2 (data not shown). In contrast, deletion of the PxIxIT motif had no effect on Slm1 or Slm2 interaction with Avo2 as measured using the two-hybrid technique (data not shown). Thus, for both Slm1 and Slm2, we defined a small PxIxIT-related motif required specifically for their interaction with calcineurin.

For other substrates, eliminating the calcineurin-docking site abolishes their calcineurin-dependent dephosphorylation. Hence, we investigated the effect of deleting the PxIxIT motif in Slm1 and Slm2. We expressed Slm1$^{\Delta PNIYIQ}$ and Slm2$^{\Delta PEFYIE}$ as GST-fusion proteins in cells lacking endogenous Slm1 and Slm2 (Fig.2C). In contrast to the wild type GST-Slm2 and GST-Slm1, the GST-Slm2$^{\Delta PEFYIE}$ and GST-Slm1$^{\Delta PNIYIQ}$ showed no difference in electrophoretic

mobility or extent of phosphorylation in extracts of cells containing or lacking calcineurin. Furthermore, it was evident that in contrast to GST-Slm2, GST-Slm2$^{\Delta PEFYIE}$ accumulated in the phosphorylated form even in cells containing calcineurin. We observed a similar behavior for GST-Slm1$^{\Delta PNIYIQ}$, however the differences were less striking due to the partial effects of calcineurin on Slm1 dephosphorylation. We conclude from these findings that calcineurin binding to Slm1 and Slm2 via their PxIxIT motif is required for calcineurin-dependent dephosphorylation of these proteins, and that GST-Slm1$^{\Delta PNIYIQ}$ and GST-Slm2$^{\Delta PEFYIE}$ are hyperphosphorylated *in vivo*.

Next, we tested whether the PxIxIT-related motif was required for Slm protein function or localization. *SLM1* and *SLM2* are redundant for an essential function (4). Therefore, to test the ability of different *SLM* alleles to support growth, we introduced them into a *slm1Δ slm2Δ* strain that also contained a *URA3* CEN plasmid, expressing *SLM2* from its own promoter (pGB013). We then tested whether the different strains could grow in the absence of pGB013 (i.e. on plates containing 5FOA) (Fig. 2D). As expected, cells expressing the vector alone were not able to grow, confirming that *SLM1* and *SLM2* form an essential gene pair. Wild type *SLM1* and *SLM2* as well as their PxIxIT-deleted counterparts were able to promote growth with similar efficiencies. This shows that calcineurin-dependent regulation of Slm1 and Slm2 is dispensable for growth under standard conditions. Calcineurin is essential for yeast growth under certain stress conditions, including ionic stress (Na^+, Li^+, Mn^{2+}, Ca^{2+}), high pH or in the presence of cell-wall disrupting drugs (cacofluorowhite and congo red). However, no growth defects were observed for the strains expressing PxIxIT-deleted *SLM1* and *SLM2* alleles under any of these stress conditions (data not shown). Slm1 and Slm2 localize to punctate patches at the cell surface (4, 27) and GFP-Slm proteins lacking the PxIxIT motif displayed an identical localization (Fig. 2E). In addition, Slm1 and Slm2 are required for polarization of the actin cytoskeleton. We used Texas Red-phalloidin to visualize cellular actin in budded yeast cells and observed no

differences in actin cytoskeleton organization between cells expressing either wild type Slm1 or Slm2 or the corresponding mutant proteins lacking the calcineurin-docking site (Fig. 2E).

Thus, calcineurin-dependent regulation of Slm1 and Slm2 is not required for their ability to support growth, to localize to the cell periphery or to polarize the actin cytoskeleton.

Slm1 and Slm2 are dephosphorylated by calcineurin during heat stress and after addition of sphingolipids.

During heat stress, Slm1 is transiently dephosphorylated and subsequently re-phosphorylated (4). Hence, we tested the effect of calcineurin on Slm protein phosphorylation under these conditions. We expressed Slm1 and Slm2 and their PxIxIT-deleted counterparts Slm1$^{\Delta PNIYIQ}$ and Slm2$^{\Delta PEFYIE}$ as GST-fusion proteins in the strain lacking endogenous Slm1 and Slm2 (Fig. 3). Shifting cells from 25 ^{o}C to 37 ºC induced no detectable change in the phosphorylation of GST-Slm2 and resulted in a slight increase in net phosphorylation of GST-Slm1 after 75 minutes (20% increase). However, the effect of heat stress on phosphorylation of GST-Slm1 and GST-Slm2 became much more apparent when calcineurin activity was inhibited with the specific inhibitor, FK506, or when the calcineurin-docking site of GST-Slm1 or GST-Slm2 was deleted. Following a shift from 25 ^{o}C to 37 ^{o}C, we found a time-dependent increase in the phosphorylation of GST-Slm2 purified from cells treated with FK506, and of purified GST-Slm2$^{\Delta PEFYIE}$ (~10-fold increase in both cases, Fig3A). Phosphorylation of GST-Slm1 purified from cells treated with FK506 and of purified GST-Slm1$^{\Delta PNIYIQ}$ also increased after a shift to high temperature, although the magnitude of the change was smaller (~2 - 3-fold, Fig 3B).

Heat stress transiently increases biosynthesis of sphingoid bases (phytosphingosine and dihydrosphingosine), which in turn activate downstream kinases (21, 44). Therefore, we tested whether the addition of phytosphingosine could mimic the effect of elevated temperature to promote phosphorylation GST-Slm1$^{\Delta PNIYIQ}$ and GST-Slm2$^{\Delta PEFYIE}$ (Fig. 4). Indeed, as observed for

heat stress (Fig.3), addition of 20 μM phytosphingosine to cells at 25 °C increased the phosphorylation of GST- Slm2$^{\Delta PEFYIE}$ (~10 fold increase, Fig. 4A) and GST- Slm1$^{\Delta PNIYIQ}$ (~2 fold increase, Fig. 4B). Together, these results indicate that through increased synthesis of phytosphingosine, heat stress triggers an increase in Slm1 and Slm2 phosphorylation that is largely counteracted *in vivo* by calcineurin-mediated dephosphorylation.

These data suggest that both elevated temperature and addition of phytosphingosine lead to activation of calcineurin *in vivo*, and consequently to increased Slm protein dephosphorylation. We therefore tested the effects of heat stress and phytosphingosine on calcineurin by monitoring the activity of Crz1, a calcineurin-regulated transcription factor. We measured expression of a 4xCDRE::lacZ reporter gene, which is specifically activated by Crz1 (65). Table 3 shows that elevated temperature as well as the addition of phytosphingosine (20 μM) increased Crz1 activity, and that this increased activity was completely inhibited by FK506. Thus, the increase in Crz1 activity reflects activation of calcineurin in response to heat stress or incubation with phytosphingosine.

A previous study showed that Slm1 is phosphorylated by the TORC2 protein kinase (4). If heat stress activates phosphorylation of Slm1 and Slm2 by TORC2, and this TORC2-mediated phosphorylation is reversed by calcineurin, then in *tor2^{ts}* cells we should observe no increase in Slm1 or Slm2 phosphorylation following exposure to high temperature even in cells devoid of calcineurin activity. To test this hypothesis, we shifted wild-type or *tor2^{ts}* cells to 37 °C, and then induced synthesis of either GST-Slm1 or GST-Slm2. As we observed earlier (Fig.3), GST-Slm2 phosphorylation was undetectable in wild-type or *tor2^{ts}* cells at 25 °C, and GST-Slm1 displayed a basal level of phosphorylation that was identical in wild-type and *tor2^{ts}* cells (Fig. 5). We also examined GST-Slm1 and GST-Slm2 phosphorylation in cells shifted to high temperature in the presence of the calcineurin inhibitor, FK506. As expected, phosphorylation of both proteins increased as a result of exposure to high temperature, and we observed the same level of phosphorylation in wild-type and *tor2^{ts}* FK506-treated cells (Fig. 5).

Thus, these findings suggest that heat stress causes an increase in Slm1 and Slm2 phosphorylation that is Tor2p-independent and counteracted by calcineurin.

Because heat stress-induced phosphorylation of Slm1 and Slm2 was mimicked by addition of phytosphingosine (Fig 4), we tested whether the increased phosphorylation of GST-Slm1$^{\Delta PNIYIQ}$ and GST-Slm2$^{\Delta PEFYIE}$ at high temperature was prevented by the addition of myriocin, a potent inhibitor of the serine palmitoyltransferase responsible for catalyzing the first step in the biosynthesis of sphingolipids. Indeed, we found that more than 90% of the heat stress-induced phosphorylation of GST-Slm1$^{\Delta PNIYIQ}$ and GST-Slm2$^{\Delta PEFYIE}$ was inhibited by myriocin (Fig. 6A), indicating that this increase in phosphorylation of Slm proteins is dependent on the *de novo* sphingolipid biosynthesis. In addition, these results suggest that sphingolipid-dependent protein kinases are responsible for the increase in Slm1 and Slm2 phosphorylation observed (Fig. 3). We also investigated the effect of myriocin on the steady state level of GST-Slm1$^{\Delta PNIYIQ}$ and GST-Slm2$^{\Delta PEFYIE}$ phosphorylation in cells grown at three different temperatures: 25 ^{o}C, 30 ^{o}C, and 37 ^{o}C (Fig. 6B). First, we observed that the overall level of both GST-Slm1$^{\Delta PNIYIQ}$ and GST-Slm2$^{\Delta PEFYIE}$ phosphorylation increased with temperature. Phosphorylation of GST-Slm2$^{\Delta PEFYIE}$, was extremely low at 25 ^{o}C and increased dramatically with temperature. GST-Slm1$^{\Delta PNIYIQ}$ was phosphorylated at all temperatures, but showed increased phosphorylation, especially at 37 ^{o}C. Second, at each temperature where phosphorylation was detected, it was decreased by addition of myriocin. We made similar observations for GST-Slm1 and GST-Slm2 in myriocin-treated cells lacking calcineurin (*cnb1Δ*) (data not shown). Thus, under all conditions tested, phosphorylation of Slm1 and Slm2 is dependent on *de novo* biosynthesis of sphingoid bases.

Slm1 and Slm2 activity determines sensitivity to myriocin.

We then investigated whether Slm1 and Slm2 play a physiological role in sphingolipid signaling and/or metabolism. Sphingolipids are essential for yeast cell growth and survival. Here

we used myriocin to investigate growth phenotypes related to deletion or overexpression of *SLM1* and *SLM2* (Fig. 7). Because Slm1 and Slm2 phosphorylation varied with temperature, we also examined growth at two different temperatures: 30 ^{o}C and 37 ^{o}C. First, we found that all strains tested were more sensitive to growth inhibition by myriocin at 37 ºC than at 30 ºC, which necessitated the use of lower myriocin concentrations at high temperature (Fig 7 A, B and C; compare left and right panels). Second, we found that strains lacking either *SLM1* or *SLM2* showed increased sensitivity to myriocin at both temperatures (Fig. 7A). A stronger effect was observed for deletion of *SLM1*, which is more highly expressed than *SLM2* (4). In contrast, we found that *slm1Δ* cells were more resistant to aureobasidin A (Fig. 7A), which inhibits Aur1, an enzyme responsible for the production of the inositolphosphorylceramide, a complex sphingolipid (37). Incubation of cells with aureobasidin A can lead to the cellular accumulation of intermediates in the sphingolipid biosynthesis pathway, including phytosphingosine and ceramide (59). We also increased Slm1 and Slm2 levels by expressing *SLM1* or *SLM2* from a CEN-based plasmid under the control of their own promoters. We found that elevating *SLM1* and *SLM2* copy number conferred resistance to myriocin at either 30 ^{o}C or 37 ^{o}C (Fig. 7B). Taken together, these data implicate Slm1 and Slm2 in sphingolipid metabolism and/or signaling. We then tested whether the presence or the absence of the calcineurin-binding site on Slm1 and Slm2 affected resistance to myriocin (Fig. 7C). At 30 ^{o}C, cells expressing *SLM1*$^{\Delta PNIYIQ}$ were more sensitive to myriocin than cells expressing *SLM1*, while surprisingly, at 37 ^{o}C there was no difference in the growth of these two strains over a range of myriocin concentrations (Fig 7B and data not shown). Similarly, cells expressing *SLM2*$^{\Delta PEFYIE}$ were more sensitive to myriocin than cells expressing *SLM2*. In this case, however, the difference in growth was more dramatic at 37 ^{o}C than at 30 ^{o}C. We observed equivalent effects on growth using cells that expressed GFP-tagged versions of these proteins, and determined that the expression level of the GFP-tagged proteins was unaffected by the presence or absence of the calcineurin

binding site (data not shown). Thus, we conclude that the growth differences described above reflect calcineurin-dependent differences in Slm protein activity *in vivo*.

These data show that, when cellular levels of sphingolipids are reduced, Slm protein activity becomes rate limiting for yeast growth, and suggests that dephosphorylation of Slm1 and Slm2 by calcineurin is necessary for these proteins to be fully functional.

Slm proteins may act downstream of phytosphingosine.

The observation that *slm1Δ* cells are both more sensitive to myriocin and more resistant to aureobasidin A than wild type cells, suggests that Slm proteins may be effectors of an intermediate in the sphingolipid biosynthesis pathway, such as phytosphingosine. However, our results do not rule out a role for Slm proteins in regulating sphingolipid levels. In order to address the potential role of Slm proteins upstream of sphingolipids, we investigated whether an external source of phytosphingosine promotes cell growth in the absence of functional Slm proteins. Addition of phytosphingosine (up to 20 μM) to the growth medium did not overcome the growth defect of *slm1^{ts} slm2Δ* cells at the non-permissive temperature (38.5 ^{o}C)(Fig. 8), suggesting that these cells are defective in sphingolipid-mediated cellular processes rather than in sphingolipid production. In contrast, exogenously added phytosphingosine overcame the myriocin-induced growth defect of wild-type cells at 38.5 ^{o}C (Fig. 8), indicating that phytosphingosine is able to promote growth in the absence of *de novo* sphingolipid biosynthesis at this high temperature. In addition, we observed that phytosphingosine restores the myriocin-induced growth inhibition in *slm1Δ* cells as well as *slm2Δ* cells, indicating that either Slm1 or Slm2 protein can mediate the growth promoting effect of phytosphingosine. Taken together, these results are consistent with a role for Slm proteins acting downstream of phytosphingosine.

Slm proteins are required for heat stress-induced endocytosis of the Fur4 uracil permease.

Increased phytosphingosine levels disrupt yeast cell growth by inhibiting nutrient uptake, including the import of tryptophan, uracil, leucine and histidine (14). The mechanism of this inhibition has been elucidated for the uracil permease, Fur4, which undergoes ubiquitin-dependent endocytosis and transport to the vacuole, where it undergoes proteolysis. This degradation of Fur4 also occurs in response to heat stress (73) and is mediated by a specific increase in phytosphingosine (13). We compared Fur4 turnover in wild-type cells (SEY6210.1) and in *slm1*^{ts} *slm2Δ* cells (AAY1623.2) during heat stress (Fig. 9). Since endogenous Fur4 levels are too low to detect by Western blotting, we over-expressed Fur4 in these cells. Cells were grown to log phase and shifted from 25 ºC to 40 ºC. This temperature was used as the heat-stress condition in these experiments because Fur4 turnover was more dramatic at 40 ^{o}C compared to 37 ^{o}C in this strain background. However, we observed the same trends in Fur4 turnover at both temperatures (data not shown). In wild-type cells, heat stress induced a time-dependent decrease in Fur4 protein levels, which is consistent with previous results (13, 73). In contrast, Fur4 levels were stable during prolonged incubation at high temperature in *slm1*^{ts} *slm2Δ* cells (Fig. 9A). This demonstrates that Slm proteins are required for Fur4 turnover induced by heat stress. Then, we tested whether this process was modulated by the presence or absence of the calcineurin-binding site of Slm1 or Slm2. We compared the Fur4 turnover rate in *slm1Δ slm2Δ* cells, expressing GST-Slm2 or GST-Slm2$^{\Delta PEFYIE}$, and found that Fur4 was degraded more rapidly in cells expressing GST-Slm2$^{\Delta PEFYIE}$ (Fig. 9B). A similar result was obtained when cells were incubated with phytosphingosine (Fig. 9C). This indicates that heat stress-induced dephosphorylation of Slm2 by calcineurin slows the rate of Fur4 turnover. The difference observed in turnover rate may reflect an alteration in one or more steps in the ubiquitin-dependent endocytosis and trafficking of Fur4 to the vacuole. These findings suggest

that calcineurin can regulate sphingolipid-mediated processes through dephosphorylation of Slm2. However, we observed no difference in Fur4 turnover in cells expressing GST-Slm1 vs. GST-Slm1$^{\Delta PNIYIQ}$ (data not shown).

Next we examined in more detail the accumulation of Fur4 in *slm*^{ts} cells. We included cycloheximide during the incubation at high temperature to follow only the fate of presynthesized Fur4 (73). We also assayed Fur4 levels by monitoring [^{14}C]-uracil uptake (Fig 10A), which allows sensitive quantification of cell-surface Fur4, as any Fur4 in intracellular compartments will not contribute to uracil transport. As previously described, after a shift to high temperature, uracil uptake rapidly decreased in wild-type cells (73). In contrast, uracil transport activity remained high in *slm*^{ts} cells. These observations establish that internalization of Fur4 is blocked in *slm*^{ts} cells at restrictive temperature. It has been shown that, as for many membrane proteins, ubiquitination of Fur4 precedes and is required for its internalization (31). Using the anti-Fur4 antibody, we showed that in plasma membrane fractions of *slm*^{ts} cells exposed to high temperature, Fur4 accumulates in high molecular weight forms (Fig 10B). These slow-migrating forms of Fur4 were also seen in plasma membrane fractions of *act1-3* cells at restrictive temperature, which are defective for endocytosis and have been shown to accumulate ubiquitinated forms of Fur4 ((31) and Fig 10B). In contrast, high molecular weight forms of Fur4 were not observed in mutants defective for the Rsp5 ubiquitin protein ligase, which is responsible for cell surface ubiquitylation of Fur4 and many other plasma membrane proteins ((31) and Fig 10B). Membrane fractions of *slmt*^{s} and *act1-3* cells incubated at restrictive temperature also accumulated high molecular weight species that reacted with an anti-ubiquitin antibody (data not shown). Therefore, we conclude that in *slm*^{ts} cells, Fur4 accumulates at the plasma membrane in a ubiquitinated form, and that internalization is inhibited at a post-ubiquitination step.

DISCUSSION

The major finding of this study is that Slm1 and Slm2 are novel calcineurin substrates that promote yeast cell growth under sphingolipid-limiting conditions and endocytosis of a nutrient permease in response to heat stress. Interfering with calcineurin-dependent dephosphorylation of Slm proteins alters their activity *in vivo*. Thus, these studies identify a mechanism by which calcineurin may modulate sphingolipid-dependent events and establish the potential for cross-talk between these two signaling pathways.

Slm1 and Slm2 are novel calcineurin substrates.

In this study, we identify Slm1 and Slm2 as targets of the phosphatase calcineurin and show that, like other calcineurin substrates (1, 3, 18, 36, 66), Slm1 and Slm2 each contain a PxIxIT-related docking site that mediates its interaction with the A subunit of calcineurin. This interaction is essential for dephosphorylation of Slm1 and Slm2 by calcineurin, and by creating *SLM1* and *SLM2* alleles lacking their respective PxIxIT motifs, we were able to assess the contribution of calcineurin signaling to Slm1 and Slm2 function *in vivo*.

Slm1 and Slm2 bind to calcineurin with different affinities. *In vivo* yeast two-hybrid assays suggest that full-length Slm2 associates more tightly with calcineurin than Slm1, and *in vitro* assays confirm this difference (Roy, Li, Hogan and Cyert, unpublished results). Furthermore, the affinity of Slm1 and Slm2 for calcineurin correlates with the extent to which they are dephosphorylated by this phosphatase. Slm2 is completely dephosphorylated by calcineurin *in vivo* and *in vitro*, while Slm1 is only partially dephosphorylated by calcineurin.

The physiological consequences of calcineurin-mediated Slm dephosphorylation have yet to be fully elucidated. *SLM1* and *SLM2* are redundant for an essential function, which does not require calcineurin, as $SLM1^{\Delta PNIYIQ}$ and $SLM2^{\Delta PEFYIE}$ each support viability. In cells

expressing a single *SLM* allele, however, abrogating Slm2 regulation by calcineurin modifies its function: The ability of Slm2$^{\Delta PEFYIE}$ to promote growth in the presence of myriocin is compromised, and expression of this protein causes faster turnover of the Fur4 permease during heat stress. Disruption of Slm1 regulation by calcineurin also diminishes its ability to support myriocin resistance at 30 ^{o}C, but has no effect on Fur4 turnover. Taken together, these observations indicate that calcineurin can modify Slm function. However, in wild type cells, which express both Slm1 and Slm2, and in which Slm1 is the predominant protein (4), the physiological significance of this regulation is somewhat unclear. Calcineurin, which is activated under conditions of environmental stress, may modify a specific aspect of Slm function or a restricted population of Slm proteins under these conditions. Further investigation is required to establish the biochemical mechanism by which Slm proteins act, and similarly to fully appreciate the consequences of their dephosphorylation by calcineurin.

Slm proteins may act downstream of sphingoid bases.

Sphingolipids are produced via a pathway that is conserved from yeast to mammals (20, 60). They consist of a long-chain base, which is usually a linear alkane of 18 or 20 carbons having hydroxyls on C-1 and C-3 and an amino group on C-2. Yeast makes two types of long-chain bases, dihydrosphingosine and phytosphingosine. These sphingoid bases rapidly and transiently accumulate during heat stress, but are not incorporated into ceramides or complex sphingolipids (60). Rather, they act as signals to promote cellular stress responses. Importantly, addition of exogenous sphingoid bases to yeast at low temperature induces several aspects of the heat stress response, including trehalose accumulation, the expression of stress element (STRE)-controlled stress response genes, cell cycle arrest and the stimulation of ubiquitin-dependent protein turn-over (13, 21, 44, 58, 76). Sphingoid bases exert their effects at least in part by activating protein phosphorylation (12, 41, 29) .

Our data suggest a possible role for Slm proteins as mediators of sphingolipid-dependent signaling. First, phosphorylation of Slm1 and Slm2 is modulated by sphingoid bases *in vivo*. Second, Slm proteins are required for heat stress-induced turnover of the Fur4 permease, which is induced by sphingoid bases (13). Third, Slm1 and Slm2 modulate cell growth in the presence of drugs that perturb sphingolipid biosynthesis. Fourth, in contrast to *lcb1-100* cells, which are defective in the first step of sphingolipid biosynthesis (76), the lethality of cells lacking Slm protein activity is not overcome by providing an external source of phytosphingosine, suggesting that Slm proteins act downstream of this mediator.

Phosphorylation of Slm proteins is modulated by sphingolipids

The biochemical function of Slm1 and Slm2 is yet to be elucidated, however, it is clear that their activity and phosphorylation are highly regulated *in vivo*. Our studies examine modulation of Slm protein phosphorylation by sphingolipids and the protein phosphatase calcineurin, both during heat stress and growth at constant temperature. During heat stress, a major consequence of increased levels of phytosphingosine and dihydrosphingosine is to activate protein kinases. Pkh1 and Pkh2, the yeast homologs of mammalian PDK1 (12), are activated by phytosphingosine, and in turn phosphorylate and activate downstream kinases, including Ypk1, Ypk2, Pkc1, and Sch9 (12, 41, 61). Some of these kinases (Ypk1, Ypk2, Sch9) may also be stimulated directly by phytosphingosine (52). Heat stress and exogenous addition of sphingoid bases also stimulate calcineurin activity ((78) and Table 3). The mechanism for this activation must still be uncovered, but is likely to involve stimulation of Ca^{2+}-influx systems, as exposure of yeast cells to sphingosine 1-phosphate, a sphingolipid produced in mammalian cells, stimulates Ca^{2+} accumulation (8).

When cells are shifted to high temperature, the net level of Slm1 and Slm2 phosphorylation changes little over the next 75 minutes. However, during this time, there is enhanced sphingolipid-dependent phosphorylation of Slm proteins that is counteracted by

calcineurin-mediated dephosphorylation. Thus, during heat stress, the rate at which Slm1 and Slm2 cycle between their phosphorylated and dephosphorylated states must increase. Currently, it is unclear what consequence these changes in phosphorylation state have on Slm protein function. Perhaps, as for small GTP-binding proteins, the switch between two different states is an integral aspect of Slm protein activity.

Additional studies are required to establish which kinase(s) are responsible for the heat stress induced phosphorylation of Slm proteins. Kinases that are activated by phytosphingosine directly (Pkh1, Pkh2, Ypk1, Ypk2 and Sch9) or indirectly (Pkc1) are attractive candidates. A recent study showed that myriocin treatment abrogates Mss4-dependent PIP kinase activity (47) which might in turn reduce recruitment of Slm proteins to the plasma membrane, which depends on PIP_2-binding to the PH domain in each protein (4). Thus, sphingolipids may also affect Slm protein phosphorylation indirectly by modulating their localization and access to kinases, such as Tor2p, that reside at the cell periphery. Consistent with this possibility, we observed an increase in cytosolic localization of GFP-Slm1 and GFP-Slm2 in myriocin-treated cells (data not shown).

A previous study showed that TORC2 phosphorylates Slm1 *in vitro* (4). Furthermore, pulse-chase analysis of Slm1 revealed its rapid dephosphorylation after exposure to high temperature, followed by TOR2-dependent re-phosphorylation. The timing of these events parallel the transient de-localization of the actin cytoskeleton in response to heat stress. In contrast, by analyzing steady-state phosphorylation of the entire cellular pool of Slm1 and Slm2, we observe a heat stress-induced increase in phosphorylation, when calcineurin is inactivated, that is independent of Tor2p and occurs over a prolonged time period (≥75 min). These kinetics are more similar to that of downstream events like endocytosis of Fur4, which continues ≥120 minutes following a shift to high temperature. It is likely, then, that multiple phosphorylation events occur, with both Tor2p and sphingolipid-regulated kinases contributing to total phosphorylation of Slm proteins during heat stress and potentially playing quite different roles in

Slm regulation. Sphingolipid-dependent phosphorylation of Slm1 and Slm2 that is counteracted by calcineurin is also observed in cells grown under constant conditions, with the extent of Slm phosphorylation increasing with temperature. Thus similar processes may underlie Slm protein phosphorylation during both normal and stress conditions.

Slm proteins are required for heat stress-induced Fur4 endocytosis.

Sphingolipids inhibit nutrient import during heat stress by promoting degradation of nutrient permeases, including the uracil permease, Fur4, and the general amino acid permease, Gap1 (13, 14). This degradation depends on the *de novo* biosynthesis of sphingolipids and is mimicked by addition of exogenous phytosphingosine (13). Slm proteins are required for heat stress-induced Fur4 turnover, which occurs through ubiquitination, internalization, and trafficking of the permease to the vacuole (25, 26, 30, 31). Ubiquitinated Fur4 accumulates at the surface of *slm1*^{ts} cells, indicating that Slm proteins are required for internalization of Fur4. The actin cytoskeleton is required for the internalization step of endocytosis; many mutants with defects in actin organization or actin-binding proteins are unable to carry out endocytosis and accumulate ubiquitylated forms of Fur4 at the cell surface (31, 46, 57). Furthermore, mutants that lack components of the endocytosis machinery, such as the amphiphysin homologs, Rvs161 and Rvs167, are defective for actin polarization (54). *slm1*^{ts} cells show defects in both actin cytoskeleton polarization (4) and endocytosis, and may therefore participate directly in either or both of these processes.

A role for sphingolipid signaling in endocytosis has been clearly demonstrated by studies of *lcb1-100* cells, which, at restrictive temperature, are unable to carry out the first step in sphingolipid biosynthesis. These cells display defects in endocytosis and actin organization, which are remediated by addition of phytosphingosine or overexpression of sphingolipid-regulated kinases (29, 76). The functions of Lcb1 and Slm proteins in endocytosis, however seem distinct. In contrast to *lcb1-100*, *slm1*^{ts} cells are able to accumulate lucifer yellow-

carbohydrazide at restrictive temperature, indicating that Slm proteins are not generally required for endocytosis (data not shown). In addition, *lcb1-100* cells, at least under some growth conditions, display no defect in stress-induced endocytosis of Fur4 (24). Thus, the defect in Fur4 endocytosis observed in *slm1*^{ts} cells may reflect a specific requirement for the Slm proteins in stress-induced sphingolipid-dependent protein turnover. The possibility that calcineurin may modulate this process through dephosphorylation of Slm proteins is particularly intriguing, as calcineurin regulates endocytosis in higher eukaryotes by dephosphorylating dynamin, a PH-domain containing protein, and its associated proteins (51, 64). It is possible that there are parallels between the function of yeast Slm proteins and some of these proteins.

Slm proteins are involved in sphingolipid-dependent growth.

Sphingolipids are essential for yeast cell growth (22), and drugs that inhibit different steps of the sphingolipid biosynthesis pathway act as potent anti-fungal compounds (60). Myriocin inhibits the first step of sphingolipid biosynthesis, whereas aureobasidin A acts later in the pathway, blocking the inositol phosphorylceramide synthase, and causing depletion of complex sphingolipids, such as mannysolated inositolphosphorylceramides, and accumulation of sphingolipid intermediates, such as phytosphingosine. We demonstrate that modifying *SLM* gene copy number has pronounced effects on cell growth at both standard (30 ^{o}C) and elevated (37 ^{o}C) temperature when sphingolipid biosynthesis is inhibited. These findings suggest that Slm proteins modify the levels of sphingolipids in cells and/or are required to carry out sphingolipid-dependent cellular functions. A full understanding of the role of Slm proteins in sphinglipid signaling and metabolism awaits further characterization of the biochemical mechanism by which Slms function. However, because addition of phytosphingosine fails to rescue the growth of *slm1*^{ts} *slm2Δ* cells at restrictive temperature, we propose that Slm1 and Slm2 are downstream mediators of sphingolipid function. Furthermore, the finding that *slm1Δ* mutants are both sensitive to myriocin, and more resistant than wild-type cells to aureobasidin A

is consistent with a role for Slm proteins acting downstream of sphingolipid bases rather than complex sphingolipids.

A model for Slm function during heat stress.

During stress, cell survival depends on integrating the responses of a variety of signaling pathways, each of which monitor a distinct aspect of cell physiology. While many questions remain concerning the mechanism by which Slm proteins act, they seem to represent a key regulatory step (Fig. 11). During heat stress, Mss4 activity and concomitant PIP_2 levels are increased, thereby recruiting Slm proteins to the cell periphery, where they are phosphorylated by the TORC2 kinase complex, which further stabilizes their localization. We show here that Slm proteins are similarly affected by heat stress and sphingoid bases, which rapidly and transiently accumulate during heat stress. Both thermal stress and phytosphingosine cause increased phosphorylation of Slm proteins (via unknown kinases) and simultaneously activate their dephosphorylation by calcineurin. All of these regulatory pathways, Mss4/PIP_2, TORC2, sphingolipids and calcineurin, independently contribute to cell survival during stress and impinge on Slm protein function. Furthermore, Slm proteins are required for polarization of the actin cytoskeleton (4, 27) and for endocytosis of the uracil permease, Fur4, during heat stress. A direct role for Slm1 and Slm2 in either actin organization or endocytosis could explain both of these defects. We cannot rule out, however, the possibility that these defects occur as an indirect consequence of disrupting Slm function. Future experiments will aim to elucidate the biochemical function of these proteins and to determine the role that phosphorylation plays in modulating their activity.

ACKNOWLEDGEMENTS

We thank Scott Emr for generously providing *slm1*^{ts} cells, for helpful discussion, and for communicating experimental results prior to publication. We thank F. Roelants and J. Thorner for helpful discussions, and all members of the Cyert laboratory for both technical advice and useful discussions. We thank J. Roy for critically reading the manuscript. Funding for this work was provided by NIH research grant GM-48729 to MSC. G.B. is a postdoctoral fellow of the Fund for Scientific Research Flanders (Fonds voor Wetenschappelijk Onderzoek Vlaanderen) and was recipient of a postdoctoral fellowship for Biomedical Research in the U.S.A. funded by the D. Collen Research Foundation vzw and Belgian American Educational Foundation. Work performed in RHT's lab is supported by the Centre National de la Recherche Scinetifique (CNRS), by a grant from the Association pour la Recherche contre le Cancer (ARC) (grant n°3298), and by a special grant from the Ministère de la Recherche (ACI BSMC).

REFERENCES

1. **Aramburu, J., F. Garcia-Cozar, A. Raghavan, H. Okamura, A. Rao, and P. G. Hogan.** 1998. Selective inhibition of NFAT activation by a peptide spanning the calcineurin targeting site of NFAT. Mol Cell **1:**627-37.
2. **Aramburu, J., A. Rao, and C. B. Klee.** 2000. Calcineurin: from structure to function. Curr Top Cell Regul **36:**237-95.
3. **Aramburu, J., M. B. Yaffe, C. Lopez-Rodriguez, L. C. Cantley, P. G. Hogan, and A. Rao.** 1999. Affinity-driven peptide selection of an NFAT inhibitor more selective than cyclosporin A. Science **285:**2129-33.
4. **Audhya, A., R. Loewith, A. B. Parsons, L. Gao, M. Tabuchi, H. Zhou, C. Boone, M. N. Hall, and S. D. Emr.** 2004. Genome-wide lethality screen identifies new PI4,5P(2) effectors that regulate the actin cytoskeleton. Embo J **23:**3747-57.
5. **Ausubel, F., R. E. Brent R., K. R.E., M. R.E., J. G. Seidman, S. J.A., and S. Struhl.** 1987. Current protocols in molecular biology. Wiley, New York, N.Y.
6. **Bartel, P. L., C.-T. Chien, R. Sternglanz, and S. Fields.** 1993. Using the two-hybrid system to detect protein-protein interactions. Cellular Interactions in Development: A practical Approach (Hartley, D.A. ed.) **Oxford University Press:**153-179.
7. **Bassel-Duby, R., and E. N. Olson.** 2003. Role of calcineurin in striated muscle: development, adaptation, and disease. Biochem Biophys Res Commun **311:**1133-41.
8. **Birchwood, C. J., J. D. Saba, R. C. Dickson, and K. W. Cunningham.** 2001. Calcium influx and signaling in yeast stimulated by intracellular sphingosine 1-phosphate accumulation. J Biol Chem **276:**11712-8.
9. **Blondel, M. O., J. Morvan, S. Dupre, D. Urban-Grimal, R. Haguenauer-Tsapis, and C. Volland.** 2004. Direct sorting of the yeast uracil permease to the endosomal system is controlled by uracil binding and Rsp5p-dependent ubiquitylation. Mol Biol Cell **15:**883-95.
10. **Boustany, L. M., and M. S. Cyert.** 2002. Calcineurin-dependent regulation of Crz1 nuclear export requires Msn5p and a conserved calcineurin docking site. Genes Dev **16:**608-19.
11. **Bultynck, G., E. Vermassen, K. Szlufcik, P. De Smet, R. A. Fissore, G. Callewaert, L. Missiaen, H. De Smedt, and J. B. Parys.** 2003. Calcineurin and intracellular Ca2+-release channels: regulation or association? Biochem Biophys Res Commun **311:**1181-93.
12. **Casamayor, A., P. D. Torrance, T. Kobayashi, J. Thorner, and D. R. Alessi.** 1999. Functional counterparts of mammalian protein kinases PDK1 and SGK in budding yeast. Curr Biol **9:**186-97.
13. **Chung, N., G. Jenkins, Y. A. Hannun, J. Heitman, and L. M. Obeid.** 2000. Sphingolipids signal heat stress-induced ubiquitin-dependent proteolysis. J Biol Chem **275:**17229-32.
14. **Chung, N., C. Mao, J. Heitman, Y. A. Hannun, and L. M. Obeid.** 2001. Phytosphingosine as a specific inhibitor of growth and nutrient import in Saccharomyces cerevisiae. J Biol Chem **276:**35614-21.
15. **Cyert, M. S.** 2003. Calcineurin signaling in Saccharomyces cerevisiae: how yeast go crazy in response to stress. Biochem Biophys Res Commun **311:**1143-50.
16. **Cyert, M. S., R. Kunisawa, D. Kaim, and J. Thorner.** 1991. Yeast has homologs (CNA1 and CNA2 gene products) of mammalian calcineurin, a calmodulin-regulated phosphoprotein phosphatase. Proc Natl Acad Sci U S A **88:**7376-80.
17. **Cyert, M. S., and J. Thorner.** 1992. Regulatory subunit (CNB1 gene product) of yeast Ca2+/calmodulin-dependent phosphoprotein phosphatases is required for adaptation to pheromone. Mol Cell Biol **12:**3460-9.

18. **Dell'Acqua, M. L., K. L. Dodge, S. J. Tavalin, and J. D. Scott.** 2002. Mapping the protein phosphatase-2B anchoring site on AKAP79. Binding and inhibition of phosphatase activity are mediated by residues 315-360. J Biol Chem **277:**48796-802.
19. **Desrivieres, S., F. T. Cooke, P. J. Parker, and M. N. Hall.** 1998. MSS4, a phosphatidylinositol-4-phosphate 5-kinase required for organization of the actin cytoskeleton in Saccharomyces cerevisiae. J Biol Chem **273:**15787-93.
20. **Dickson, R. C., and R. L. Lester.** 2002. Sphingolipid functions in Saccharomyces cerevisiae. Biochim Biophys Acta **1583:**13-25.
21. **Dickson, R. C., E. E. Nagiec, M. Skrzypek, P. Tillman, G. B. Wells, and R. L. Lester.** 1997. Sphingolipids are potential heat stress signals in Saccharomyces. J Biol Chem **272:**30196-200.
22. **Dickson, R. C., G. B. Wells, A. Schmidt, and R. L. Lester.** 1990. Isolation of mutant Saccharomyces cerevisiae strains that survive without sphingolipids. Mol Cell Biol **10:**2176-81.
23. **Dupre, S., and R. Haguenauer-Tsapis.** 2001. Deubiquitination step in the endocytic pathway of yeast plasma membrane proteins: crucial role of Doa4p ubiquitin isopeptidase. Mol Cell Biol **21:**4482-94.
24. **Dupre, S., and R. Haguenauer-Tsapis.** 2003. Raft partitioning of the yeast uracil permease during trafficking along the endocytic pathway. Traffic **4:**83-96.
25. **Dupre, S., D. Urban-Grimal, and R. Haguenauer-Tsapis.** 2004. Ubiquitin and endocytic internalization in yeast and animal cells. Biochim Biophys Acta **1695:**89-111.
26. **Dupre, S., C. Volland, and R. Haguenauer-Tsapis.** 2001. Membrane transport: ubiquitylation in endosomal sorting. Curr Biol **11:**R932-4.
27. **Fadri, M., A. Daquinag, S. Wang, T. Xue, and J. Kunz.** 2005. The pleckstrin homology domain proteins Slm1 and Slm2 are required for actin cytoskeleton organization in yeast and bind phosphatidylinositol-4,5-bisphosphate and TORC2. Mol Biol Cell **16:**1883-900.
28. **Feske, S., H. Okamura, P. G. Hogan, and A. Rao.** 2003. Ca2+/calcineurin signalling in cells of the immune system. Biochem Biophys Res Commun **311:**1117-32.
29. **Friant, S., R. Lombardi, T. Schmelzle, M. N. Hall, and H. Riezman.** 2001. Sphingoid base signaling via Pkh kinases is required for endocytosis in yeast. Embo J **20:**6783-92.
30. **Galan, J. M., and R. Haguenauer-Tsapis.** 1997. Ubiquitin lys63 is involved in ubiquitination of a yeast plasma membrane protein. Embo J **16:**5847-54.
31. **Galan, J. M., V. Moreau, B. Andre, C. Volland, and R. Haguenauer-Tsapis.** 1996. Ubiquitination mediated by the Npi1p/Rsp5p ubiquitin-protein ligase is required for endocytosis of the yeast uracil permease. J Biol Chem **271:**10946-52.
32. **Goldstein, A. L., and J. H. McCusker.** 1999. Three new dominant drug resistance cassettes for gene disruption in Saccharomyces cerevisiae. Yeast **15:**1541-53.
33. **Goud, B., A. Salminen, N. C. Walworth, and P. J. Novick.** 1988. A GTP-binding protein required for secretion rapidly associates with secretory vesicles and the plasma membrane in yeast. Cell **53:**753-68.
34. **Groth, R. D., R. L. Dunbar, and P. G. Mermelstein.** 2003. Calcineurin regulation of neuronal plasticity. Biochem Biophys Res Commun **311:**1159-71.
35. **Harper, J. W., G. R. Adami, N. Wei, K. Keyomarsi, and S. J. Elledge.** 1993. The p21 Cdk-interacting protein Cip1 is a potent inhibitor of G1 cyclin-dependent kinases. Cell **75:**805-16.
36. **Heath, V. L., S. L. Shaw, S. Roy, and M. S. Cyert.** 2004. Hph1p and Hph2p, novel components of calcineurin-mediated stress responses in Saccharomyces cerevisiae. Eukaryot Cell **3:**695-704.
37. **Heidler, S. A., and J. A. Radding.** 1995. The AUR1 gene in Saccharomyces cerevisiae encodes dominant resistance to the antifungal agent aureobasidin A (LY295337). Antimicrob Agents Chemother **39:**2765-9.

38. **Helliwell, S. B., I. Howald, N. Barbet, and M. N. Hall.** 1998. TOR2 is part of two related signaling pathways coordinating cell growth in Saccharomyces cerevisiae. Genetics **148:**99-112.
39. **Ho, H. L., Y. S. Shiau, and M. Y. Chen.** 2005. Saccharomyces cerevisiaeTSC11/AVO3 participates in regulating cell integrity and functionally interacts with components of the Tor2 complex. Curr Genet **47:**273-88.
40. **Homma, K., S. Terui, M. Minemura, H. Qadota, Y. Anraku, Y. Kanaho, and Y. Ohya.** 1998. Phosphatidylinositol-4-phosphate 5-kinase localized on the plasma membrane is essential for yeast cell morphogenesis. J Biol Chem **273:**15779-86.
41. **Inagaki, M., T. Schmelzle, K. Yamaguchi, K. Irie, M. N. Hall, and K. Matsumoto.** 1999. PDK1 homologs activate the Pkc1-mitogen-activated protein kinase pathway in yeast. Mol Cell Biol **19:**8344-52.
42. **James, P.** 2001. Yeast two-hybrid vectors and strains. Methods Mol Biol **177:**41-84.
43. **James, P., J. Halladay, and E. A. Craig.** 1996. Genomic libraries and a host strain designed for highly efficient two-hybrid selection in yeast. Genetics **144:**1425-36.
44. **Jenkins, G. M., A. Richards, T. Wahl, C. Mao, L. Obeid, and Y. Hannun.** 1997. Involvement of yeast sphingolipids in the heat stress response of Saccharomyces cerevisiae. J Biol Chem **272:**32566-72.
45. **Jiang, B., and M. S. Cyert.** 1999. Identification of a novel region critical for calcineurin function in vivo and in vitro. J Biol Chem **274:**18543-51.
46. **Kaksonen, M., C. P. Toret, and D. G. Drubin.** 2005. A modular design for the clathrin- and actin-mediated endocytosis machinery. Cell **123:**305-20.
47. **Kobayashi, T., H. Takematsu, T. Yamaji, S. Hiramoto, and Y. Kozutsumi.** 2005. Disturbance of sphingolipid biosynthesis abrogates the signaling of Mss4, phosphatidylinositol-4-phosphate 5-kinase, in yeast. J Biol Chem **280:**18087-94.
48. **Kuno, T., H. Tanaka, H. Mukai, C. D. Chang, K. Hiraga, T. Miyakawa, and C. Tanaka.** 1991. cDNA cloning of a calcineurin B homolog in Saccharomyces cerevisiae. Biochem Biophys Res Commun **180:**1159-63.
49. **Kunz, J., R. Henriquez, U. Schneider, M. Deuter-Reinhard, N. R. Movva, and M. N. Hall.** 1993. Target of rapamycin in yeast, TOR2, is an essential phosphatidylinositol kinase homolog required for G1 progression. Cell **73:**585-96.
50. **Levin, D. E.** 2005. Cell wall integrity signaling in Saccharomyces cerevisiae. Microbiol Mol Biol Rev **69:**262-91.
51. **Liu, J. P., A. T. Sim, and P. J. Robinson.** 1994. Calcineurin inhibition of dynamin I GTPase activity coupled to nerve terminal depolarization. Science **265:**970-3.
52. **Liu, K., X. Zhang, R. L. Lester, and R. C. Dickson.** 2005. The sphingoid long chain base phytosphingosine activates AGC-type protein kinases in Saccharomyces cerevisiae including Ypk1, Ypk2, and Sch9. J Biol Chem **280:**22679-87.
53. **Liu, Y., S. Ishii, M. Tokai, H. Tsutsumi, O. Ohki, R. Akada, K. Tanaka, E. Tsuchiya, S. Fukui, and T. Miyakawa.** 1991. The Saccharomyces cerevisiae genes (CMP1 and CMP2) encoding calmodulin-binding proteins homologous to the catalytic subunit of mammalian protein phosphatase 2B. Mol Gen Genet **227:**52-9.
54. **Lombardi, R., and H. Riezman.** 2001. Rvs161p and Rvs167p, the two yeast amphiphysin homologs, function together in vivo. J Biol Chem **276:**6016-22.
55. **Luo, C., K. T. Shaw, A. Raghavan, J. Aramburu, F. Garcia-Cozar, B. A. Perrino, P. G. Hogan, and A. Rao.** 1996. Interaction of calcineurin with a domain of the transcription factor NFAT1 that controls nuclear import. Proc Natl Acad Sci U S A **93:**8907-12.
56. **Matheos, D. P., T. J. Kingsbury, U. S. Ahsan, and K. W. Cunningham.** 1997. Tcn1p/Crz1, a calcineurin-dependent transcription factor that differentially regulates gene expression in Saccharomyces cerevisiae. Genes Dev **11:**3445-58.

57. **Moreau, V., J. M. Galan, G. Devilliers, R. Haguenauer-Tsapis, and B. Winsor.** 1997. The yeast actin-related protein Arp2p is required for the internalization step of endocytosis. Mol Biol Cell **8:**1361-75.
58. **Munn, A. L., and H. Riezman.** 1994. Endocytosis is required for the growth of vacuolar H(+)-ATPase-defective yeast: identification of six new END genes. J Cell Biol **127:**373-86.
59. **Nagiec, M. M., E. E. Nagiec, J. A. Baltisberger, G. B. Wells, R. L. Lester, and R. C. Dickson.** 1997. Sphingolipid synthesis as a target for antifungal drugs. Complementation of the inositol phosphorylceramide synthase defect in a mutant strain of Saccharomyces cerevisiae by the AUR1 gene. J Biol Chem **272:**9809-17.
60. **Obeid, L. M., Y. Okamoto, and C. Mao.** 2002. Yeast sphingolipids: metabolism and biology. Biochim Biophys Acta **1585:**163-71.
61. **Roelants, F. M., P. D. Torrance, N. Bezman, and J. Thorner.** 2002. Pkh1 and Pkh2 differentially phosphorylate and activate Ypk1 and Ykr2 and define protein kinase modules required for maintenance of cell wall integrity. Mol Biol Cell **13:**3005-28.
62. **Sherman, F.** 1991. Getting started with yeast. Methods Enzymol **194:**3-21.
63. **Sikorski, R. S., and P. Hieter.** 1989. A system of shuttle vectors and yeast host strains designed for efficient manipulation of DNA in Saccharomyces cerevisiae. Genetics **122:**19-27.
64. **Smillie, K. J., and M. A. Cousin.** 2005. Dynamin I phosphorylation and the control of synaptic vesicle endocytosis. Biochem Soc Symp**:**87-97.
65. **Stathopoulos, A. M., and M. S. Cyert.** 1997. Calcineurin acts through the CRZ1/TCN1-encoded transcription factor to regulate gene expression in yeast. Genes Dev **11:**3432-44.
66. **Stathopoulos-Gerontides, A., J. J. Guo, and M. S. Cyert.** 1999. Yeast calcineurin regulates nuclear localization of the Crz1 transcription factor through dephosphorylation. Genes Dev **13:**798-803.
67. **Sun, L., H. D. Youn, C. Loh, M. Stolow, W. He, and J. O. Liu.** 1998. Cabin 1, a negative regulator for calcineurin signaling in T lymphocytes. Immunity **8:**703-11.
68. **Sun, Y., R. Taniguchi, D. Tanoue, T. Yamaji, H. Takematsu, K. Mori, T. Fujita, T. Kawasaki, and Y. Kozutsumi.** 2000. Sli2 (Ypk1), a homologue of mammalian protein kinase SGK, is a downstream kinase in the sphingolipid-mediated signaling pathway of yeast. Mol Cell Biol **20:**4411-9.
69. **Uetz, P., L. Giot, G. Cagney, T. A. Mansfield, R. S. Judson, J. R. Knight, D. Lockshon, V. Narayan, M. Srinivasan, P. Pochart, A. Qureshi-Emili, Y. Li, B. Godwin, D. Conover, T. Kalbfleisch, G. Vijayadamodar, M. Yang, M. Johnston, S. Fields, and J. M. Rothberg.** 2000. A comprehensive analysis of protein-protein interactions in Saccharomyces cerevisiae. Nature **403:**623-7.
70. **Urban-Grimal, D., B. Pinson, J. Chevallier, and R. Haguenauer-Tsapis.** 1995. Replacement of Lys by Glu in a transmembrane segment strongly impairs the function of the uracil permease from Saccharomyces cerevisiae. Biochem J **308 (Pt 3):**847-51.
71. **Vernet, T., D. Dignard, and D. Y. Thomas.** 1987. A family of yeast expression vectors containing the phage f1 intergenic region. Gene **52:**225-33.
72. **Volland, C., C. Garnier, and R. Haguenauer-Tsapis.** 1992. In vivo phosphorylation of the yeast uracil permease. J Biol Chem **267:**23767-71.
73. **Volland, C., D. Urban-Grimal, G. Geraud, and R. Haguenauer-Tsapis.** 1994. Endocytosis and degradation of the yeast uracil permease under adverse conditions. J Biol Chem **269:**9833-41.
74. **Yoshimoto, H., K. Saltsman, A. P. Gasch, H. X. Li, N. Ogawa, D. Botstein, P. O. Brown, and M. S. Cyert.** 2002. Genome-wide analysis of gene expression regulated by

the calcineurin/Crz1 signaling pathway in Saccharomyces cerevisiae. J Biol Chem **277:**31079-88.

75. **Yu, J. W., J. M. Mendrola, A. Audhya, S. Singh, D. Keleti, D. B. DeWald, D. Murray, S. D. Emr, and M. A. Lemmon.** 2004. Genome-wide analysis of membrane targeting by S. cerevisiae pleckstrin homology domains. Mol Cell **13:**677-88.
76. **Zanolari, B., S. Friant, K. Funato, C. Sutterlin, B. J. Stevenson, and H. Riezman.** 2000. Sphingoid base synthesis requirement for endocytosis in Saccharomyces cerevisiae. Embo J **19:**2824-33.
77. **Zhang, X., R. L. Lester, and R. C. Dickson.** 2004. Pil1p and Lsp1p negatively regulate the 3-phosphoinositide-dependent protein kinase-like kinase Pkh1 and downstream signaling pathways Pkc1 and Ypk1. J Biol Chem **279:**22030-8.
78. **Zhao, C., U. S. Jung, P. Garrett-Engele, T. Roe, M. S. Cyert, and D. E. Levin.** 1998. Temperature-induced expression of yeast FKS2 is under the dual control of protein kinase C and calcineurin. Mol Cell Biol **18:**1013-22.

Table1. Yeast strains used in this study

Strain	***Relevant genotype***	***Source or reference***
PJ69-4A	*MAT***a** trp1-901 leu2-3,112 ura3-52 his3-200 gal4Δ *gal80*Δ *GAL2-ADE2 LYS2*::*GAL1-HIS3 met2*::*GAL7-lacZ*	(43)
YPH499	*MAT***a** ura3-52 lys2-801 ade2-101 trp1 Δ*63 his3*-Δ*200 leu2*-Δl	(63)
DD12	As YPH499 except *cnb1*::*URA3*::*hisG*	(17)
BY4741	*MAT***a** *leu2*Δ *ura3*Δ *met15*Δ *his3*Δ	Open Biosystems
VHY61	MATα *leu2*Δ *ura3*Δ *met15*Δ *his3*Δ *slm2Δ::KAN*^{R}	This study
VHY66	As BY4741, *slm1Δ::KAN*^{R}	This study
GBY059	As VHY61, *slm1Δ::NAT*^{R} + pRS316-Slm2	This study
SEY6210.1	MAT**a** leu2-3 ura3-52 his3-Δ200 trp1-Δ901 lys2-801 suc2-Δ9	(4)
AAY1602	As SEY6210.1; *slm1Δ::HIS3*	(4)
AAY1610	As SEY6210.1; *slm2Δ::HIS3*	(4)
AAY1623.2	As SEY6210.1; *slm1Δ::HIS3 slm2Δ::HIS3* + pRS415-slm1-2 (LEU2 CEN6 slm1-2)	(4)
LBY66	As YPH499 except 4xCDRE:::lacZ:::TRP	Laboratory stock
JK9-3d**a**	*MAT***a** *leu2-3, 112 trp1 ura3 rme1 his4 HML***a**	(49)
SH121	JK9-3d**a** *ade2 tor2::ADE2*/YPplac111::*tor2-21*	(38)
NY13	*MAT***a** *ura3-52 gal2*	(33)
NY279	*MAT***a** *act1-3 ura3-52 gal2*	(33)
FY56	*MATα his4-912δ lys2-128δ ura3-52*	Fred Winston
FW1808	*MATα rsp5-1 his4-912δ lys2-128δ ura3-52*	Fred Winston
GBY030	YPH499 + pRD56-Slm2	This study
GBY031	YPH499 + pRD56-Slm1	This study
GBY032	DD12 + pRD56-Slm2	This study
GBY033	DD12 + pRD56-Slm1	This study
GBY115	As VHY61, *slm1Δ::NAT*^{R} + pRD56-Slm2	This study
GBY116	As VHY61, *slm1Δ::NAT*^{R} + pRD56-Slm2$^{\Delta PEFYIE}$	This study
GBY117	As VHY61, *slm1Δ::NAT*^{R} + pRD56-Slm1	This study
GBY118	As VHY61, *slm1Δ::NAT*^{R} + pRD56-Slm1$^{\Delta PNIYIQ}$	This study
GBY152	As GBY059 + pRS313	This study
GBY153	As GBY059 + pRS313-Slm2	This study
GBY154	As GBY059 + pRS313-Slm2$^{\Delta PEFYIE}$	This study
GBY155	As GBY059 + pRS313-Slm1	This study
GBY156	As GBY059 + pRS313-Slm1$^{\Delta PNIYIQ}$	This study
GBY100	As VHY61, *slm1Δ::NAT*^{R} + pRS313-Slm2	This study
GBY101	As VHY61, *slm1Δ::NAT*^{R} + pRS313-Slm2$^{\Delta PEFYIE}$	This study
GBY102	As VHY61, *slm1Δ::NAT*^{R} + pRS313-Slm1	This study
GBY103	As VHY61, *slm1Δ::NAT*^{R} + pRS313-Slm1$^{\Delta PNIYIQ}$	This study
GBY104	As VHY61, *slm1Δ::NAT*^{R} + pUG34-Slm2	This study
GBY105	As VHY61, *slm1Δ::NAT*^{R} + pUG34-Slm2$^{\Delta PEFYIE}$	This study
GBY106	As VHY61, *slm1Δ::NAT*^{R} + pUG34-Slm1	This study
GBY107	As VHY61, *slm1Δ::NAT*^{R} + pUG34-Slm1$^{\Delta PNIYIQ}$	This study
GBY160	BY4741 + pRS313	This study
GBY161	BY4741 + pRS313-Slm2	This study
GBY162	BY4741 + pRS313-Slm1	This study
GBY179	SEY6210.1 + pVTu-Fur4	This study
GBY180	AAY1623.2 + pVTu-Fur4	This study
GBY181	GBY115 + pVTl-Fur4	This study
GBY182	GBY116 + pVTl-Fur4	This study
GBY183	GBY117 + pVTl-Fur4	This study
GBY184	GBY118 + pVTl-Fur4	This study

Table 2. Plasmids used in this study

Plasmid	*Vector*	*Insert/ORF*	*Source or reference*
	pGBT9		(6)
	pACT2		(35)
	pRD56		Gift from R. Deshaies
	pRS316		(63)
	pRS313		(63)
	pUG34		gift of U Güldener and J. H. Hegemann
	pVT102-U		(71)
BJP2014	pGBT9	$GAL4^{DBD}$-CNA1	(45)
pVH7	pGBT9	$GAL4^{DBD}$-CNA2	(36)
pGB003	pACT2	$GAL4^{AD}$-SLM2	This study
pGB004	pACT2	$GAL4^{AD}$-SLM1	This study
pGB005	pACT2	$GAL4^{AD}$-$SLM2^{\Delta PEFYIE}$	This study
pGB006	pACT2	$GAL4^{AD}$-$SLM1^{\Delta PNIYIQ}$	This study
pGB007	pRD56	GST-SLM2	This study
pGB008	pRD56	GST-$SLM2^{\Delta PEFYIE}$	This study
pGB009	pRD56	GST-SLM1	This study
pGB010	pRD56	GST-$SLM1^{\Delta PNIYIQ}$	This study
pGB013	pRS316	SLM2	This study
pGB017	pRS313	SLM2	This study
pGB018	pRS313	$SLM2^{\Delta PEFYIE}$	This study
pGB019	pRS313	SLM1	This study
pGB020	pRS313	$SLM1^{\Delta PNIYIQ}$	This study
pGB029	pUG34	GFP-SLM2	This study
pGB030	pUG34	GFP-$SLM2^{\Delta PEFYIE}$	This study
pGB031	pUG34	GFP-SLM1	This study
pGB032	pUG34	GFP-$SLM1^{\Delta PNIYIQ}$	This study
pfF	pJDB207	FUR4	(72)
pGB047	pVT102-U	FUR4	This study

.

	β-galactosidase activity (U / μg protein)	
FK506	**-**	**+**
Control (30 ºC)	0.29 ± 0.05	0.29 ± 0.04
Heat stress (from 25 ºC to 37 ºC)	1.37 ± 0.145	0.11 ± 0.06
Phytosphingosine (25 ºC)	3.93 ± 0.178	0.38 ± 0.12
Phytosphingosine (30 ºC)	7.51 ± 0.51	0.29 ± 0.11

Table 3. Heat stress and phytosphingosine causes calcineurin-dependent 4xCDRE:::lacZ expression. Strain LBY66 containing the lacZ reporter gene under the control of 4 copies of the 24-bp Calcineurin Downstream Response Element in its genome was grown in YPD under different conditions in the absence or presence of FK506 (2 μg/ml). After reaching log phase, cells were triggered with either no stress (control) or a heat stress for 3 h or 20 μM phytosphingosine for 3h at the indicated temperatures and β-galactosidase activity was assayed in cell lysates. Values represent the mean specific β-galactosidase activity, obtained from two independent experiments each performed in triplicate.

FIGURE LEGENDS

Figure 1. Slm1 and Slm2 interact with and are dephosphorylated by calcineurin. (A) Slm1 and Slm2 interact with Cna1 and Cna2 in yeast two-hybrid assays. A strain (PJ69-4A) containing *GAL1-HIS3*, *GAL2-ADE2* and *GAL7*-lacZ reporter genes was transformed with combinations of GAL4 DNA-binding domain fusions of *CNA1* and *CNA2* (DBD) and GAL4 activation domain fusions of *SLM1* and *SLM2* (AD), as indicated. Serial dilutions of saturated cultures were plated on synthetic medium containing histidine and adenine (+his+ade) or lacking histidine (-his) or lacking (-ade), and incubated for 3 days at 30 °C. β−galactosidase activity in the different strains was measured in liquid cultures, performed as described in Materials and Methods, and reported as units/μg of protein. (B) Slm1 and Slm2 are both dephosphorylated *in vivo* by calcineurin. Wild-type cells (WT, YPH499) and cells lacking the B-subunit of calcineurin *(cnb1*Δ, DD12) expressing GST-Slm2 (GBY030 and GBY032) or GST-Slm1 (GBY031 and GBY033) were grown to log phase. GST-fusion proteins were purified from extracts, subjected to SDS-PAGE and Western blotted with anti-phospho or anti-GST antibody. (C) Slm1 and Slm2 are both dephosphorylated *in vitro* by calcineurin. GST-Slm1 (GBY032) and GST-Slm2 (GBY033) purified from *cnb1*Δ cells were treated with recombinant calcineurin, calmodulin (CaM), $CaCl_2$, EGTA or λ-phosphatase as indicated in the left-hand lanes (see Materials and Methods). These samples, together with untreated GST-Slm1 and GST-Slm2 purified from *cnb1*Δ cells, were then subjected to SDS-PAGE and Western blotted with anti-phospho and anti-GST antibodies.

Figure 2. Calcineurin interacts with Slm1 and Slm2 via a C-terminal PxIxIT related motif. (A) Mapping of the calcineurin-docking site on Slm1 and Slm2 via yeast-two hybrid assays. The PJ69-4A strain containing the GAL4 DNA-binding domain fusion of *CNA1* was transformed with different truncations or internal deletions of *SLM1* and *SLM2*. Positive interactions were

identified as growth on synthetic medium lacking histidine (3 days at 30 °C). GAL4-AD fusions that interacted with Cna1 are indicated as "+", and those that did not interact are indicated as "-". (B) Relevant part of the amino acid sequence of Slm2 and Slm1 with the conserved calcineurin-docking site, a PxIxIT-related motif, underlined. (C) Deletion of the calcineurin-docking site abolishes the calcineurin-dependent dephosphorylation of Slm1 and Slm2. Wild-type GST-Slm2 (GBY115) and GST-Slm1 (GBY117) and their counterparts lacking the calcineurin-docking site, GST-Slm2$^{\Delta PEFYIE}$ (GBY116) and GST-Slm1$^{\Delta PNIYIQ}$ (GBY118) were expressed in a strain deleted for *slm1*Δ and *slm2*Δ. Cells were grown in selective synthetic medium supplemented with 4% raffinose. One culture was treated with FK506 (as indicated). GST-fusion proteins were purified from cell extracts, subjected to SDS-PAGE and Western blotted with anti-phospho and anti-GST antibodies. (D) Deletion of the calcineurin-docking site in *SLM1* or *SLM2* does not impair growth. A *slm1Δ slm2Δ* strain, expressing *SLM2* under the control of its own promoter on a pRS316 plasmid (GBY059) was transformed with either pRS313 (vector; GBY152), pRS313-Slm2 (Slm2; GBY153), pRS313-Slm2$^{\Delta PEFYIE}$ (Slm2$^{\Delta PEFYIE}$; GBY154), pRS313-Slm1 (Slm1; GBY155), pRS313-Slm1$^{\Delta PNIYIQ}$ (Slm1$^{\Delta PNIYIQ}$; GBY156). Serial dilutions of saturated cell cultures were plated on synthetic medium lacking uracil and histidine (-ura-his) and on synthetic medium lacking histidine but supplemented with 5FOA (-his+5FOA). Cells were grown for 3 days at 30 ºC. (E) Localization of Slm proteins and actin cytoskeleton stabilization by Slm proteins are not dependent on the calcineurin-docking site. *slm1Δ slm2Δ* cells expressing GFP-Slm2 (GBY104), GFP-Slm2$^{\Delta PEFYIE}$ (GBY105), GFP-Slm1 (GBY106) or GFP-Slm1$^{\Delta PNIYIQ}$ (GBY107) were grown to log phase and visualized by differential interference microscopy (DIC) and by fluorescence microscopy (GFP). Actin cytoskeleton was visualized with Texas Red-X phalloidin (TR-phalloidin) in formaldehyde-fixed cells.

Figure 3. Phosphorylation of Slm1 and Slm2 is increased during heat stress when their calcineurin-dependent dephosphorylation is compromised. (A) GST-Slm2 (GBY115) and

GST-Slm2$^{\Delta PEFYIE}$ (GBY116) were expressed in a strain lacking *slm1* and *slm2*. Cells were grown at 25°C in selective synthetic medium and expression was induced with 2% galactose. One culture was treated with FK506 (2 μg/ml) as indicated. Cells were shifted to 37 °C and samples were taken at indicated time points. GST-fusion proteins were purified from cell extracts and subjected to SDS-PAGE and Western blotting with anti-phospho and anti-GST antibodies. Immunoreactive bands were quantified using Image J software. The ratio of the anti-phospho signal over the anti-GST signal was plotted in arbitrary units (A.U.) as a function of time. (B) A similar approach as described in (A) was taken for GST-Slm1 (GBY117) and GST-Slm1$^{\Delta PNIYIQ}$ (GBY118).

Figure 4. Phytosphingosine mimics the heat stress-induced phosphorylation of Slm1 and Slm2. GST-Slm2 (GBY115), GST-Slm2$^{\Delta PEFYIE}$ (GBY116), GST-Slm1 (GBY117) and GST-Slm1$^{\Delta PNIYIQ}$ (GBY118) were expressed in a strain lacking *slm1* and *slm2*. Cells were grown at 25 °C in selective synthetic medium and expression was induced with 2% galactose. Samples were taken just before the addition of 20 μM phytosphingosine (0 min), and 45, 90 and 120 minutes after the addition of phytosphingosine. GST-fusion proteins were purified from cell extracts and subjected to SDS-PAGE and Western blotting with anti-phospho and anti-GST antibodies. Immunoreactive bands were quantified as described in Materials and Methods. The ratio of the anti-phospho signal over the anti-GST signal was plotted in arbitrary units (A.U.).

Figure 5. The heat stress-induced increase in Slm1 and Slm2 phosphorylation is independent of Tor2p. Overnight cultures of wild-type (JK9-3da) and *tor2^{ts}* (SH121) cells expressing either GST-Slm2 or GST-Slm1 were diluted to an OD_{600} of 0.2 and grown at 25 ºC for 4 hours. To one set of cultures, FK506 (2 μg/ml final concentration) or solvent (90% ethanol / 10% Tween-20) was added and cells were shifted to 38 ºC. After 30 min, galactose (2%) was added to induce protein expression and cells were grown for another 4 hours at 38 ºC. GST-

fusion proteins were purified from cell extracts and subjected to SDS-PAGE and Western blotting with anti-phospho and anti-GST antibodies.

Figure 6. Myriocin inhibits phosphorylation of Slm1 and Slm2 during heat stress and steady-state growth conditions. GST-Slm2$^{\Delta PEFYIE}$ (GBY116) and GST-Slm1$^{\Delta PNIYIQ}$ (GBY118) were expressed in a *slm1Δ slm2Δ* strain. (A) Cells were grown at 25 °C in selective synthetic medium for 4 hours and protein expression was induced with 2% galactose. Thirty minutes before the shift from 25 °C to 37 °C, myriocin (2 μg/ml) was added to one set of cultures and solvent (methanol) to the other. Samples of the different cultures were taken just before the temperature shift and 90 minutes after the shift in temperature. GST-fusion proteins were purified from cell extracts and subjected to SDS-PAGE and Western blotting with either an anti-phospho or an anti-GST antibody. (B) Cells were grown either at 25 °C, 30 °C or 37 °C in selective synthetic medium. Myriocin (2 μg/ml) was added 30 minutes before the cells were incubated with 2% galactose for 4 hours. GST-fusion proteins were purified from cell extracts and analyzed via Western immunoblotting with either an anti-phospho or an anti-GST antibody. Immunoreactive bands were quantified as described in Materials and Methods.

Figure 7. Slm1 and Slm2 modulate growth of yeast in the presence of drugs that perturb sphingolipid biosynthesis. (A) Saturated cultures of wild-type cells (BY4741) and cells lacking either *slm1* (*slm1Δ*; VHY66) or *slm2* (*slm2Δ*; VHY61) were serially diluted and spotted onto YPD, YPD plus myriocin (Myr) or YPD plus aureobasidin A (AB) and grown for 2 to 4 days at either 30 °C or 37 °C. (B) Wild-type cells containing either pRS313 (vector; GBY160) or pRS313 expressing Slm2 (GBY161) and Slm1 (GBY162) under the control of their own promoter were grown to saturation in selective synthetic medium. Saturated cultures were serially diluted and were spotted onto YPD with or without myriocin. Plates were incubated at either 30 °C or 37 °C for 2.5 days. (C) *slm1Δ slm2Δ* cells expressing Slm2 (GBY100), Slm2$^{\Delta PEFYIE}$ (GBY101), Slm1

(GBY102) or Slm1$^{\Delta PNIYIQ}$ (GBY103) under the control of their own promoter from pRS313 were grown to saturation in selective synthetic medium. Saturated cultures were serially diluted and were spotted onto YPD or YPD supplemented with 1.5 μg/ml myriocin. Cells were grown for 3 to 4 days at either 30 ºC or 37 °C as noted.

Figure 8. Slm proteins are downstream of phytosphingosine.

Saturated cultures of wild-type (SEY6210), *slm1Δ* (AAY1602), *slm2Δ* (AAY1610) and *slm1^{ts} slm2Δ* (AAY1623.2) cells were serially diluted and spotted onto YPD, YPD + 20 μM phytosphingosine (PHS), YPD + 0.4 μg/ml myriocin or YPD + 0.4 μg/ml myriocin + 20 μM phytosphingosine (PHS) and grown for 2.5 days at the indicated temperature. All plates contained 0.05% NP-40, which was used for obtaining an even distribution of phytosphingosine in the plate.

Figure 9. Slm function is required for heat shock-induced Fur4 turn-over. (A) Wild-type cells (SEY6210.1) and *slm1^{ts}slm2Δ* cells (AAY1623.2) carrying pVTu-Fur4 (GBY179 and GBY180, respectively) were shifted from 25 ^{o}C to 40 °C and samples of taken just prior to (0 min), and 15, 30, 60 minutes following heat shock. Cell lysates were analyzed by SDS-PAGE and immunoblotting with anti-Fur4 and anti-PGK antibodies. Pgk1 was used as a loading control, which also shows the absence of nonspecific protein degradation by heat shock. The left-hand numbers indicate the molecular masses of the protein standards. Immunoreactive bands were quantified as described in Materials and Methods. The ratio of the anti-Fur4 signal to the anti-Pgk1p signal is shown as a function of time. The value at 0 minutes was used as reference value and set at 100%. (B) *slm1Δ slm2Δ* cells expressing either GST-Slm2 or GST-Slm2$^{\Delta PEFYIE}$ and overexpressing Fur4 (GBY115 and GBY116, respectively) were shifted from 25 ^{o}C to 40 ^{o}C, and sampled at the indicated time points. Cell lysates were analyzed by immunoblotting and quantified as described in (A). (C) GBY115 and GBY116 were grown at 30

°C, incubated with 20 μM phytosphingosine and sampled at the indicated times. Lysates were analyzed and signals quantified as described in (A).

Figure 10. Fur4 is stabilized at the plasma membrane in the ubiquitinated form in cells lacking Slm protein activity. Wild-type cells (SEY6210.1) and *slm1^{ts}slm2Δ* cells (AAY1623.2) carrying pVTu-Fur4 (GBY179 and GBY180, respectively) were shifted to 40 °C for 10 min before adding cycloheximide (100 μg/ml). (*A),* Uracil uptake was measured at the times indicated. Results are percentages of initial activities. (*B),* Plasma membrane fractions were prepared from cycloheximide-treated cells before and 60 minutes following a shift from 25 ^{o}C to 40 ^{o}C and analyzed for uracil permease (anti-Fur4) by Western immunoblotting. Strains are as follows: left panel, WT (SEY6210.1), *slm^{ts}* (AAY1623.2); middle panel, WT (NY13), *act1-3* (NY279); right panel, WT (FY56), *rsp5^{ts}* (FW1808).

Figure 11. Regulation of actin cytoskeleton organization and nutrient permease turn-over by Slm protein functioning in response to heat stress. See text for discussion of model.

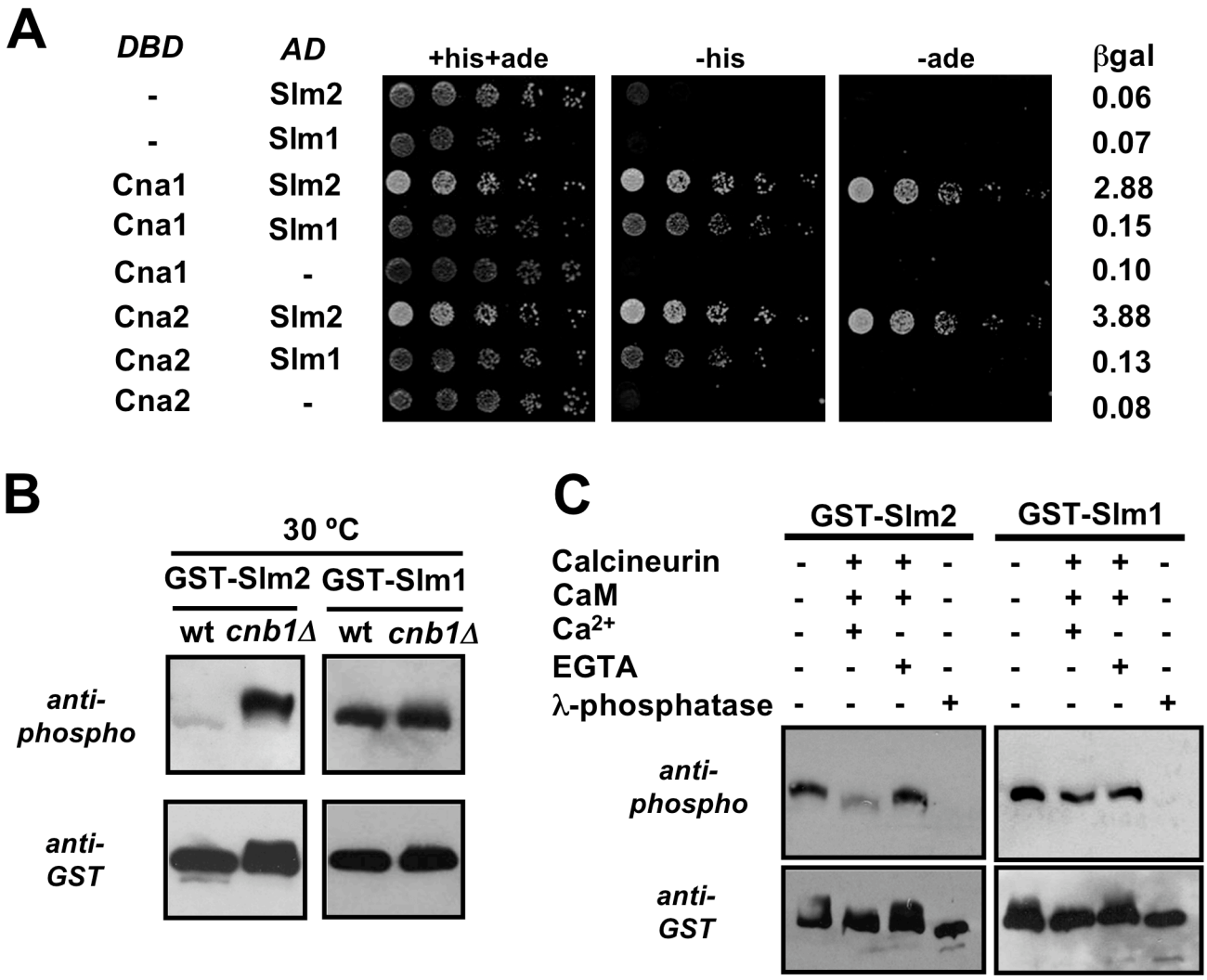
A
DBD
AD
+his+ade
-his
-ade
βgal
- Slm2 0.06
- Slm1 0.07
Cna1 Slm2 2.88
Cna1 Slm1 0.15
Cna1 - 0.10
Cna2 Slm2 3.88
Cna2 Slm1 0.13
Cna2 - 0.08
B
30 ºC
GST-Slm2
GST-Slm1
wt
cnb1Δ
wt
cnb1Δ
anti-phospho
anti-GST
C
GST-Slm2
GST-Slm1
Calcineurin
CaM
Ca2+
EGTA
λ-phosphatase
anti-phospho
anti-GST

Figure 1

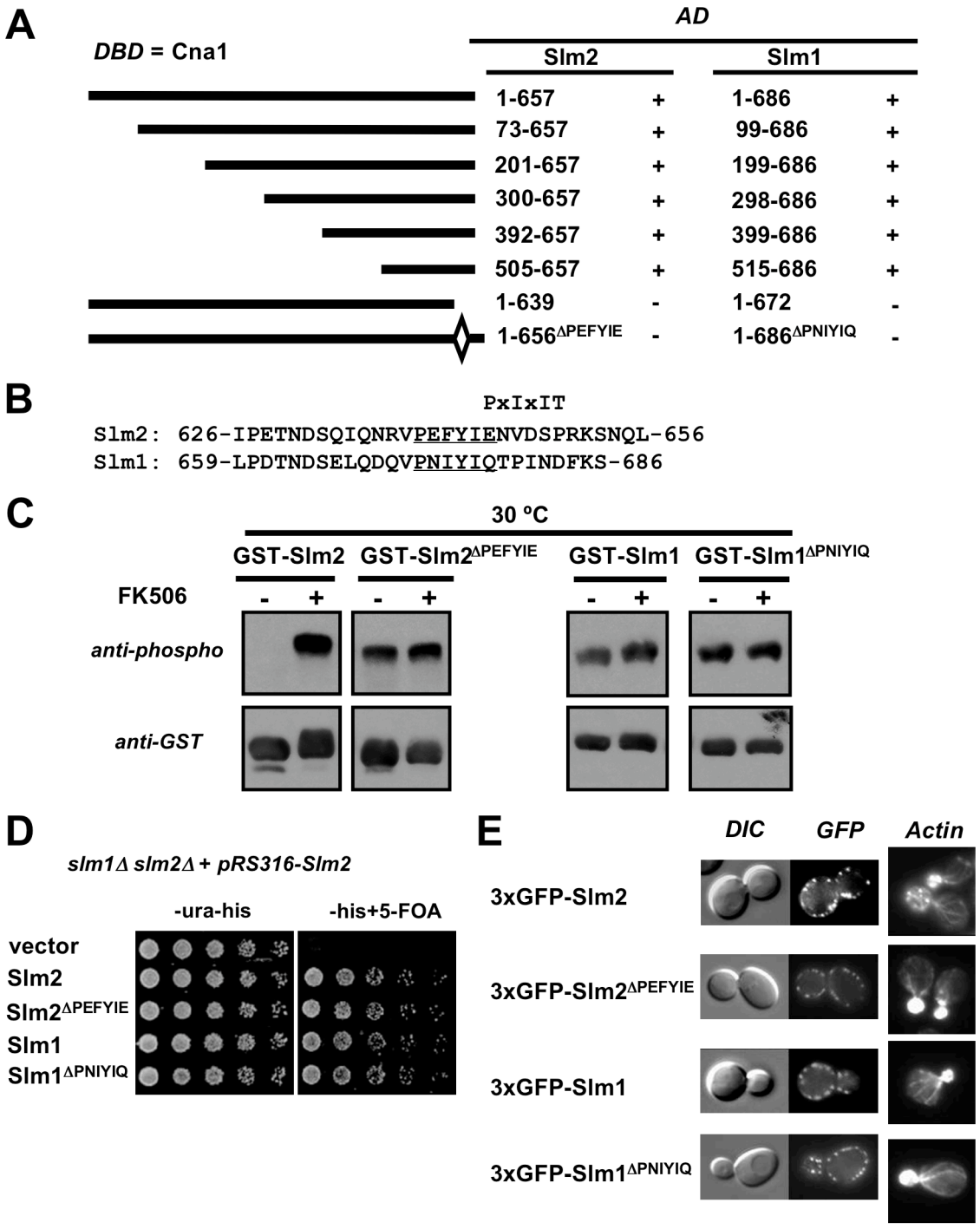
A
AD
DBD = Cna1
Slm2
Slm1
1-657 + 1-686 +
73-657 + 99-686 +
201-657 + 199-686 +
300-657 + 298-686 +
392-657 + 399-686 +
505-657 + 515-686 +
1-639 - 1-672 -
1-656ΔPEFYIE - 1-686ΔPNIYIQ -
B
PxIxIT
Slm2: 626-IPETNDSQIQNRVPEFYIENVDSPRKSNQL-656
Slm1: 659-LPDTNDSELQDQVPNIYIQTPINDFKS-686
C
30 °C
GST-Slm2
GST-Slm2ΔPEFYIE
GST-Slm1
GST-Slm1ΔPNIYIQ
FK506
- + - + - + - +
anti-phospho
anti-GST
D
slm1Δ slm2Δ + pRS316-Slm2
-ura-his
-his+5-FOA
vector
Slm2
Slm2ΔPEFYIE
Slm1
Slm1ΔPNIYIQ
E
DIC
GFP
Actin
3xGFP-Slm2
3xGFP-Slm2ΔPEFYIE
3xGFP-Slm1
3xGFP-Slm1ΔPNIYIQ

Figure 2

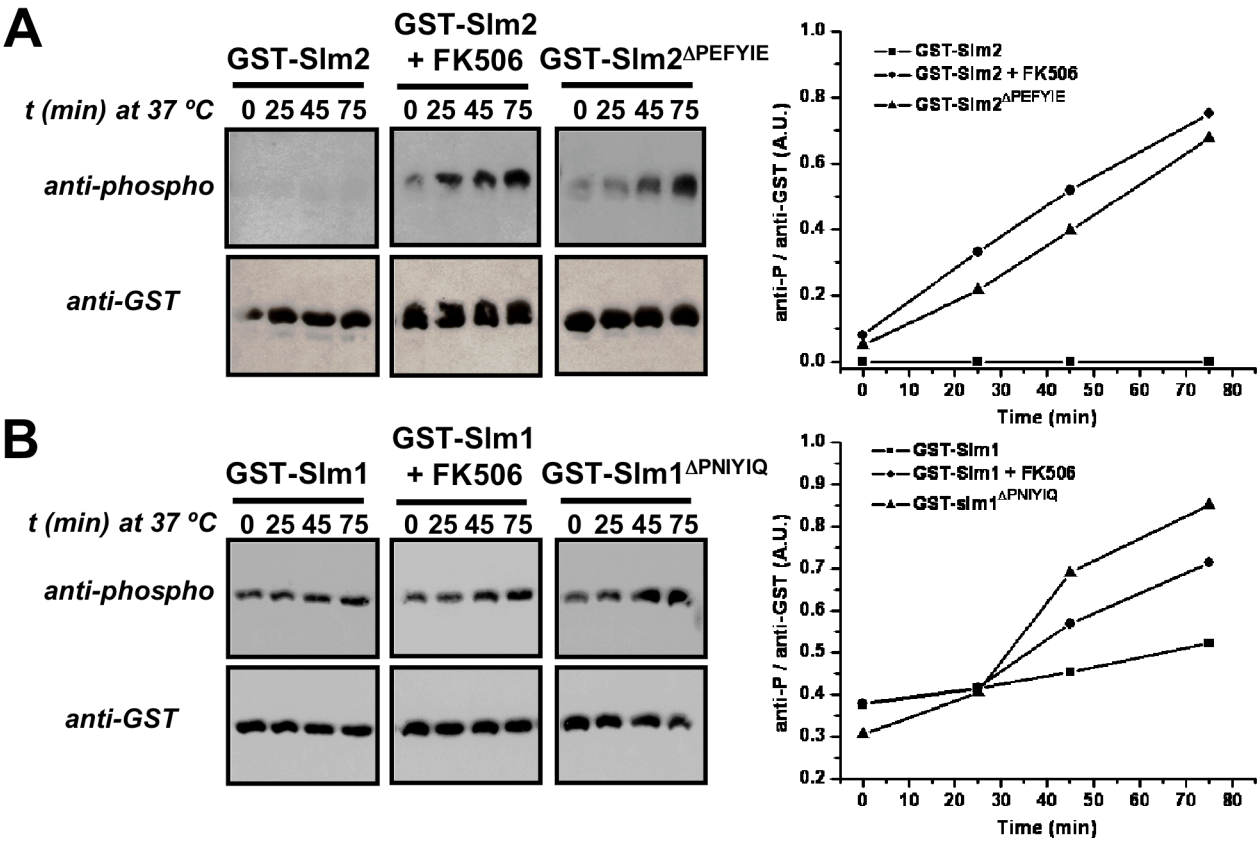
A
GST-Slm2
GST-Slm2 + FK506
GST-Slm2ΔPEFYIE
t (min) at 37 ºC
0 25 45 75
0 25 45 75
0 25 45 75
anti-phospho
anti-GST
GST-Slm2
GST-Slm2 + FK506
GST-Slm2ΔPEFYIE
anti-P / anti-GST (A.U.)
Time (min)
B
GST-Slm1
GST-Slm1 + FK506
GST-Slm1ΔPNIYIQ
t (min) at 37 ºC
0 25 45 75
0 25 45 75
0 25 45 75
anti-phospho
anti-GST
GST-Slm1
GST-Slm1 + FK506
GST-slm1ΔPNIYIQ
anti-P / anti-GST (A.U.)
Time (min)

Figure 3

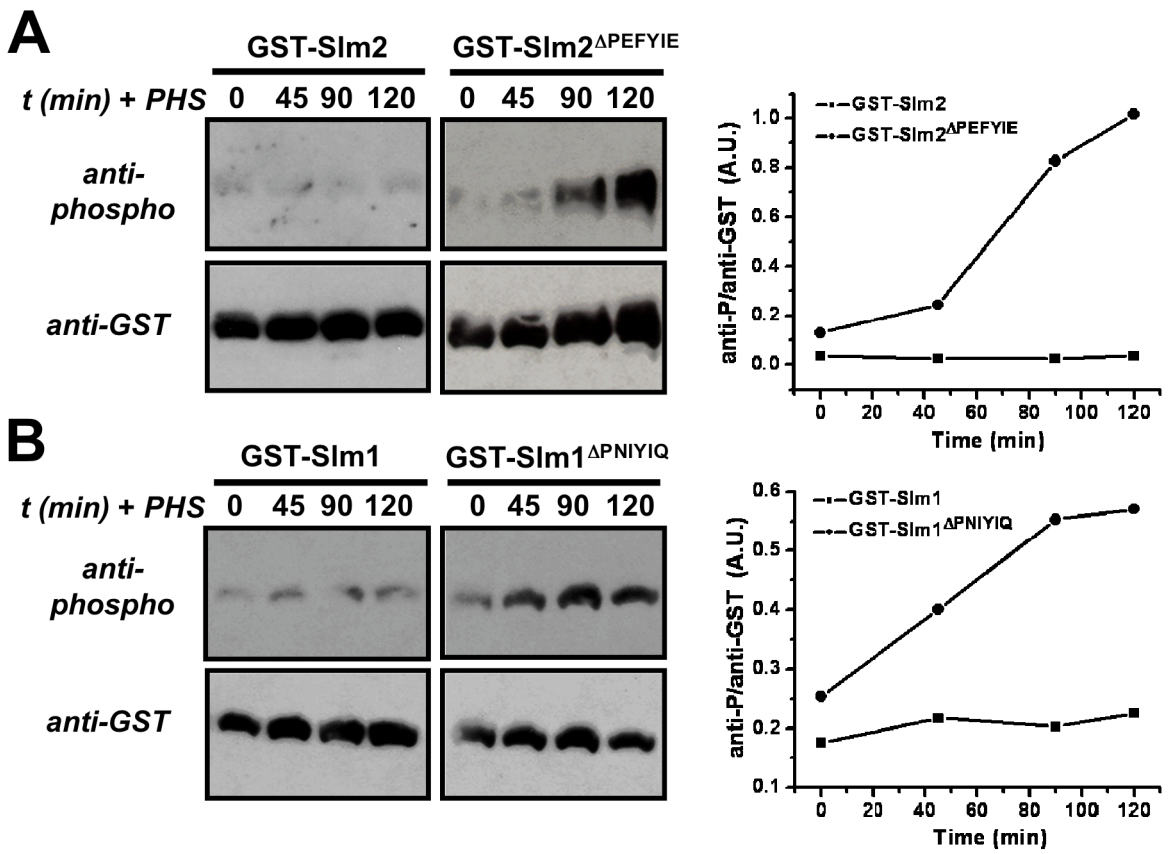
A
GST-Slm2
GST-Slm2ΔPEFYIE
t (min) + PHS 0 45 90 120 0 45 90 120
anti-phospho
anti-GST
B
GST-Slm1
GST-Slm1ΔPNIYIQ
t (min) + PHS 0 45 90 120 0 45 90 120
anti-phospho
anti-GST
GST-Slm2
GST-Slm2ΔPEFYIE
anti-P/anti-GST (A.U.)
Time (min)
GST-Slm1
GST-Slm1ΔPNIYIQ
anti-P/anti-GST (A.U.)
Time (min)

Figure 4

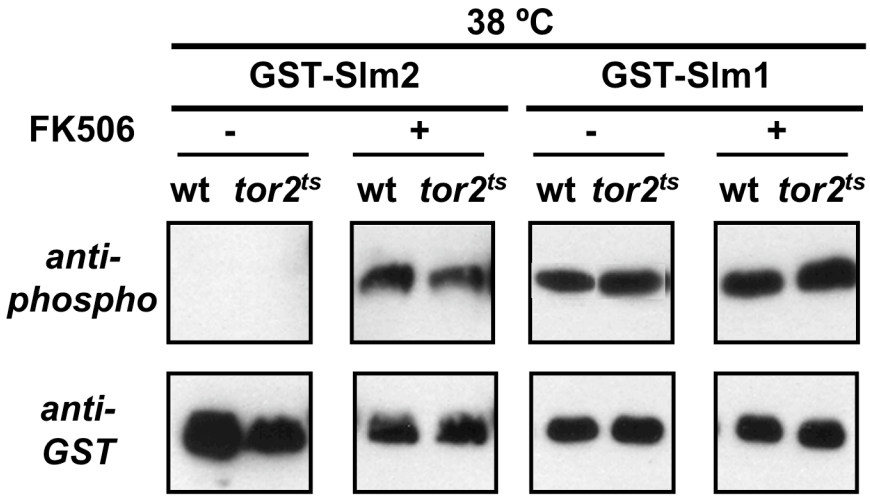
38 ºC
GST-Slm2
GST-Slm1
FK506
-
+
-
+
wt
tor2ts
wt
tor2ts
wt
tor2ts
wt
tor2ts
anti-phospho
anti-GST

Figure 5

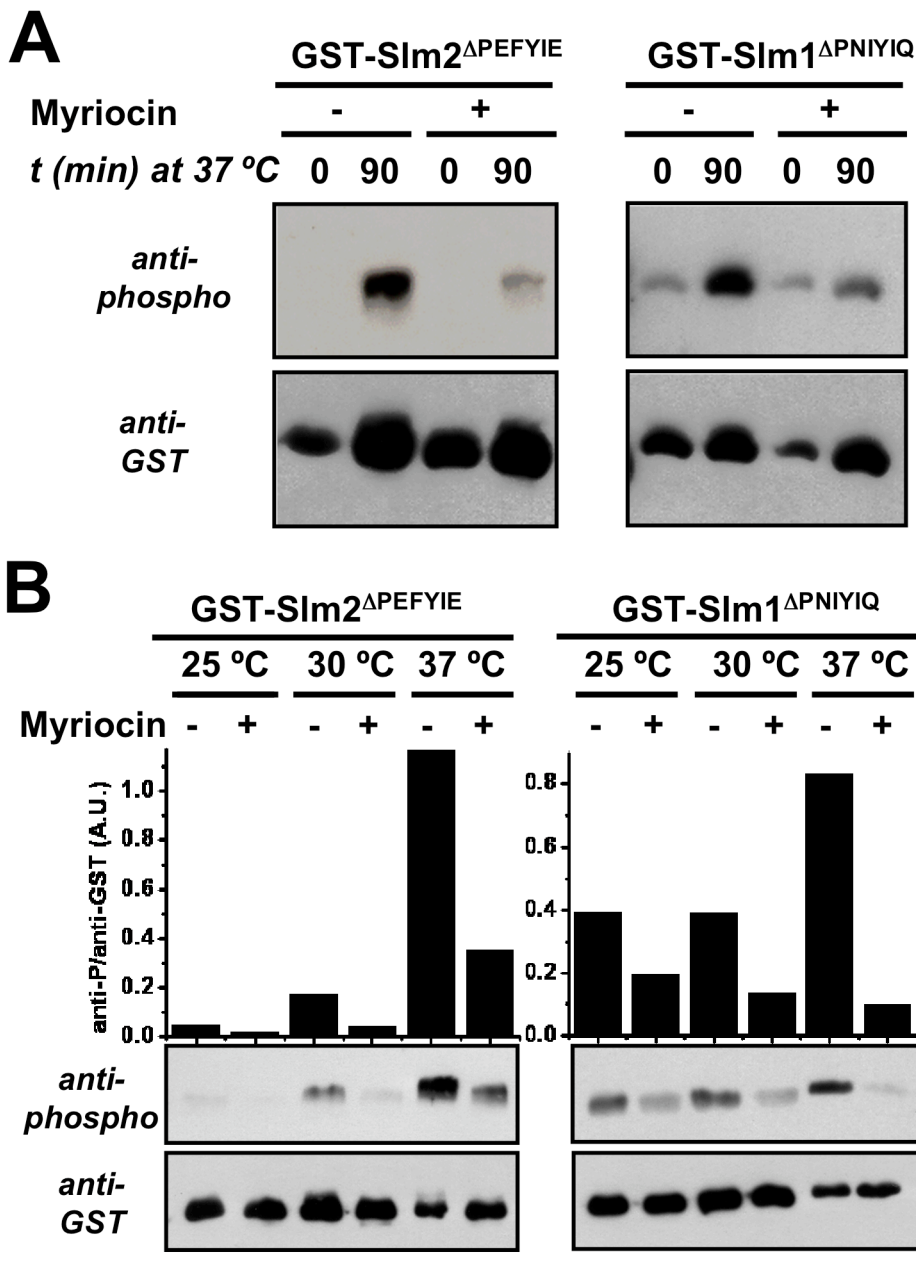
A
GST-Slm2ΔPEFYIE
GST-Slm1ΔPNIYIQ
Myriocin
-
+
-
+
t (min) at 37 ºC
0 90 0 90
0 90 0 90
anti-phospho
anti-GST
B
GST-Slm2ΔPEFYIE
GST-Slm1ΔPNIYIQ
25 ºC 30 ºC 37 ºC
25 ºC 30 ºC 37 ºC
Myriocin - + - + - +
- + - + - +
anti-P/anti-GST (A.U.)
0.0 0.2 0.4 0.6 0.8 1.0
0.0 0.2 0.4 0.6 0.8
anti-phospho
anti-GST

Figure 6

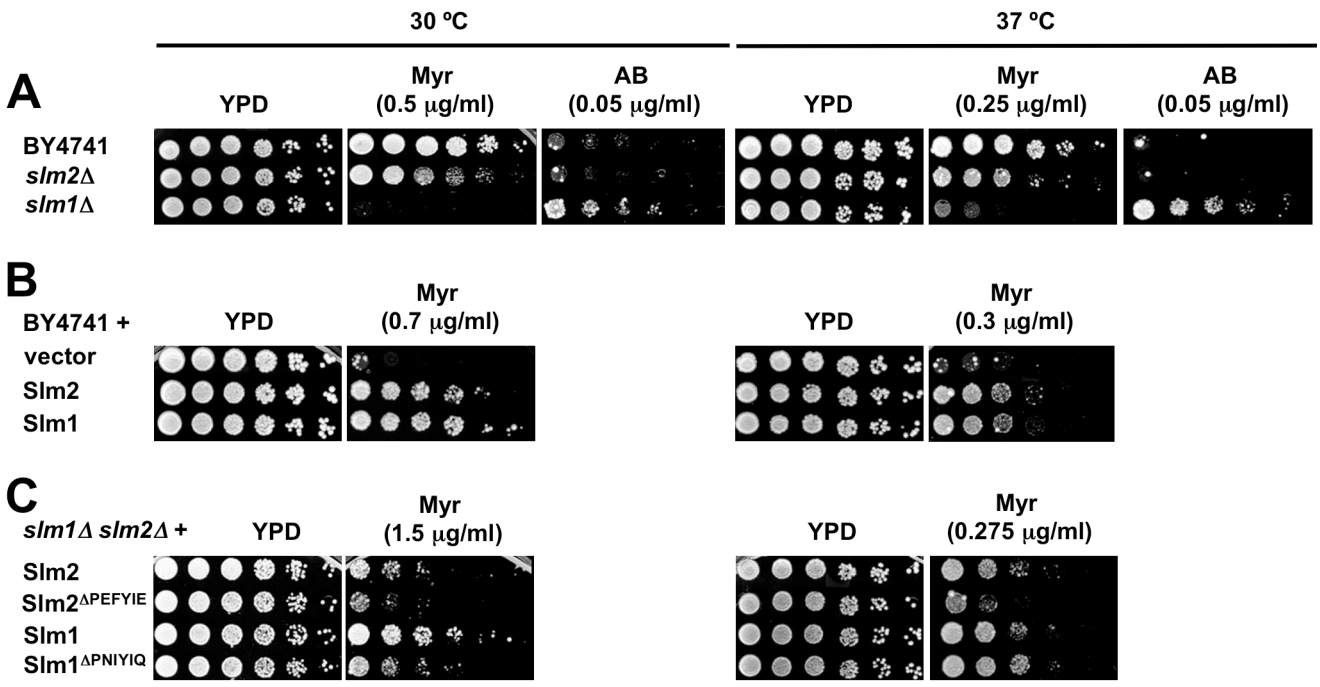
30 ºC
37 ºC
A
YPD
Myr (0.5 μg/ml)
AB (0.05 μg/ml)
YPD
Myr (0.25 μg/ml)
AB (0.05 μg/ml)
BY4741
slm2Δ
slm1Δ
B
BY4741 +
vector
Slm2
Slm1
YPD
Myr (0.7 μg/ml)
YPD
Myr (0.3 μg/ml)
C
slm1Δ slm2Δ +
Slm2
Slm2ΔPEFYIE
Slm1
Slm1ΔPNIYIQ
YPD
Myr (1.5 μg/ml)
YPD
Myr (0.275 μg/ml)

Figure 7

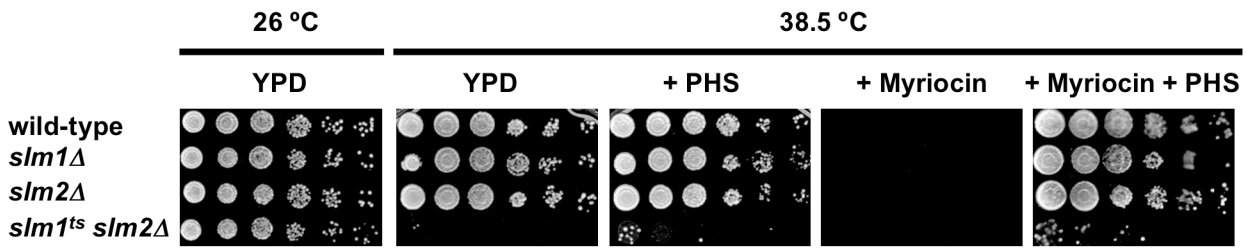
26 ºC
38.5 ºC
YPD
YPD
+ PHS
+ Myriocin
+ Myriocin + PHS
wild-type
slm1Δ
slm2Δ
slm1ts slm2Δ

Figure 8

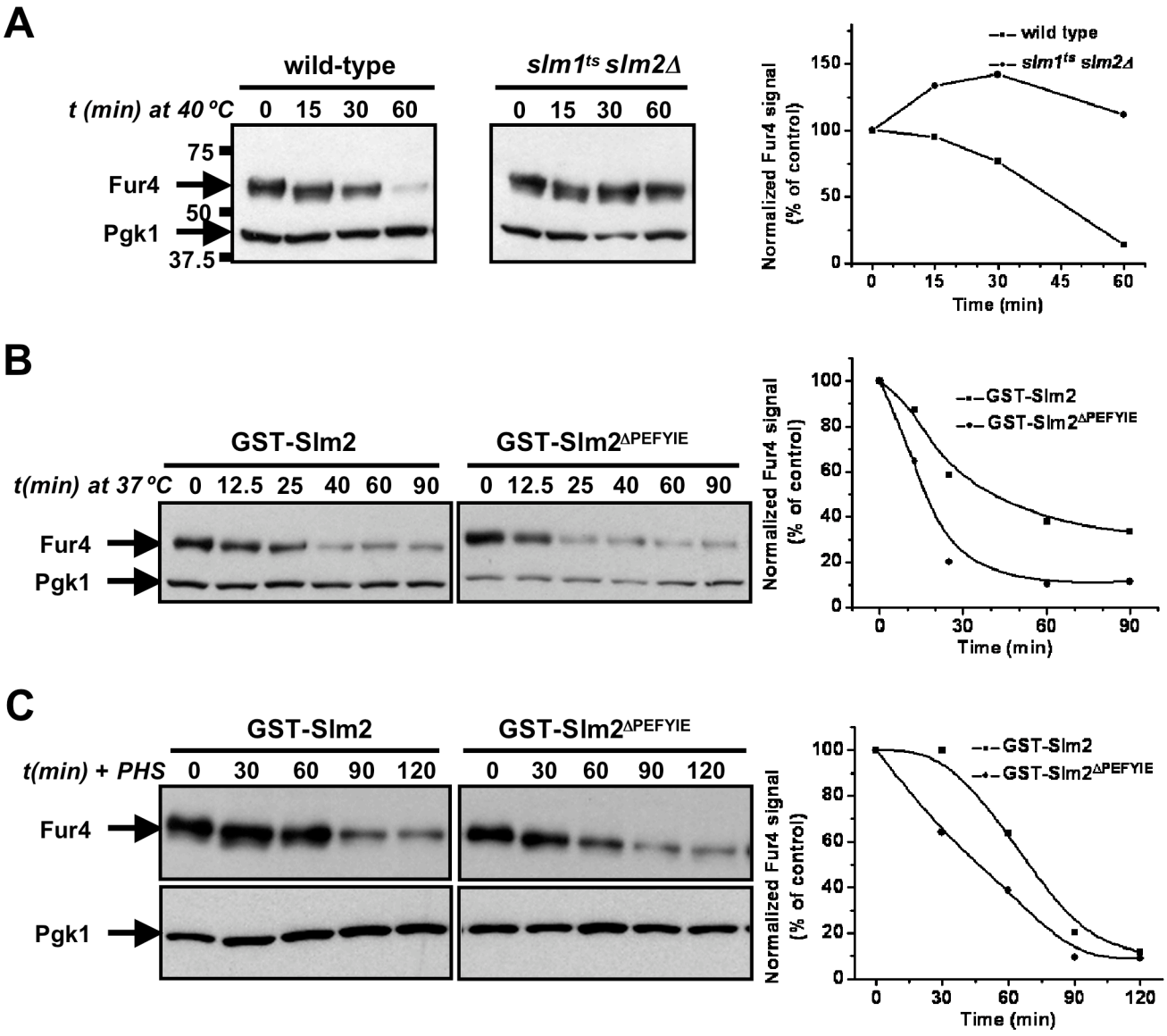
A
wild-type
slm1ts slm2Δ
t (min) at 40 °C 0 15 30 60
0 15 30 60
75
Fur4
50
Pgk1
37.5
wild type
slm1ts slm2Δ
Normalized Fur4 signal (% of control)
Time (min)
B
GST-Slm2
GST-Slm2ΔPEFYIE
t(min) at 37 °C 0 12.5 25 40 60 90
0 12.5 25 40 60 90
Fur4
Pgk1
GST-Slm2
GST-Slm2ΔPEFYIE
Normalized Fur4 signal (% of control)
Time (min)
C
GST-Slm2
GST-Slm2ΔPEFYIE
t(min) + PHS 0 30 60 90 120
0 30 60 90 120
Fur4
Pgk1
GST-Slm2
GST-Slm2ΔPEFYIE
Normalized Fur4 signal (% of control)
Time (min)

Figure 9

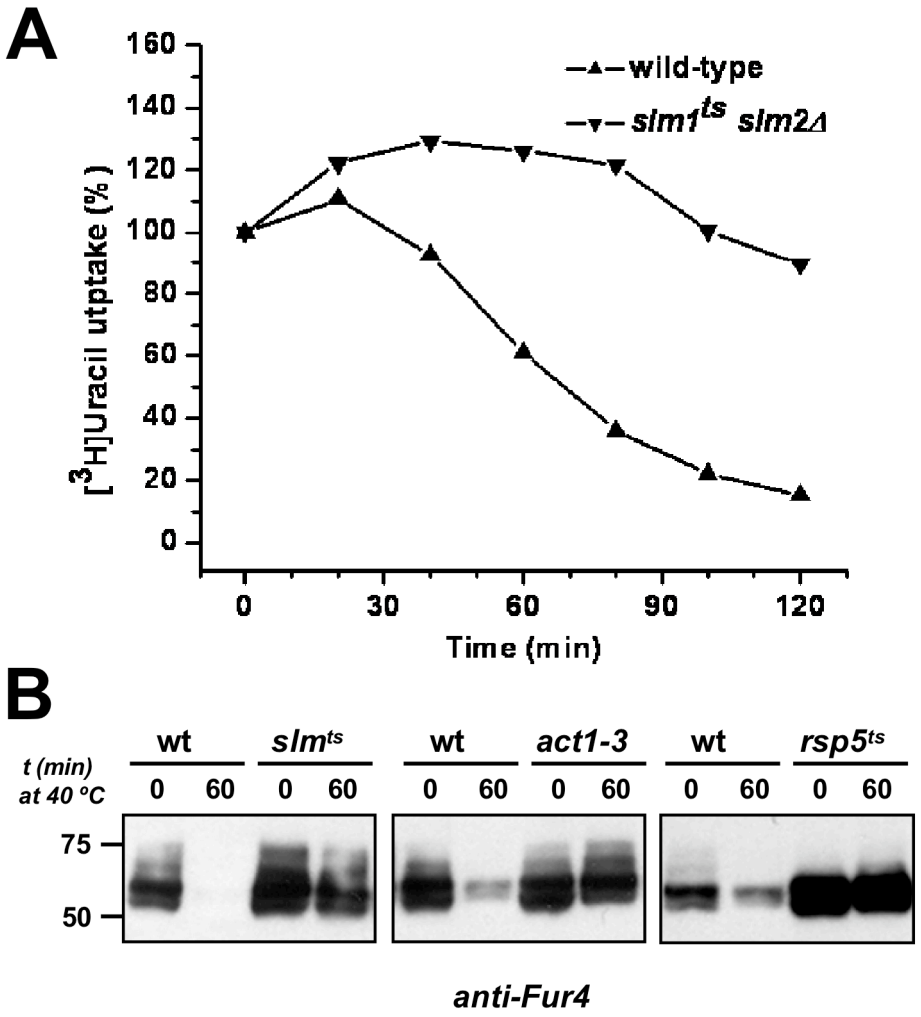
A
160
140
120
100
80
60
40
20
0
[3H]Uracil utptake (%)
wild-type
slm1ts slm2Δ
0
30
60
90
120
Time (min)
B
wt
slmts
wt
act1-3
wt
rsp5ts
t (min)
at 40 °C
0 60 0 60 0 60 0 60 0 60 0 60
75
50
anti-Fur4

Figure 10

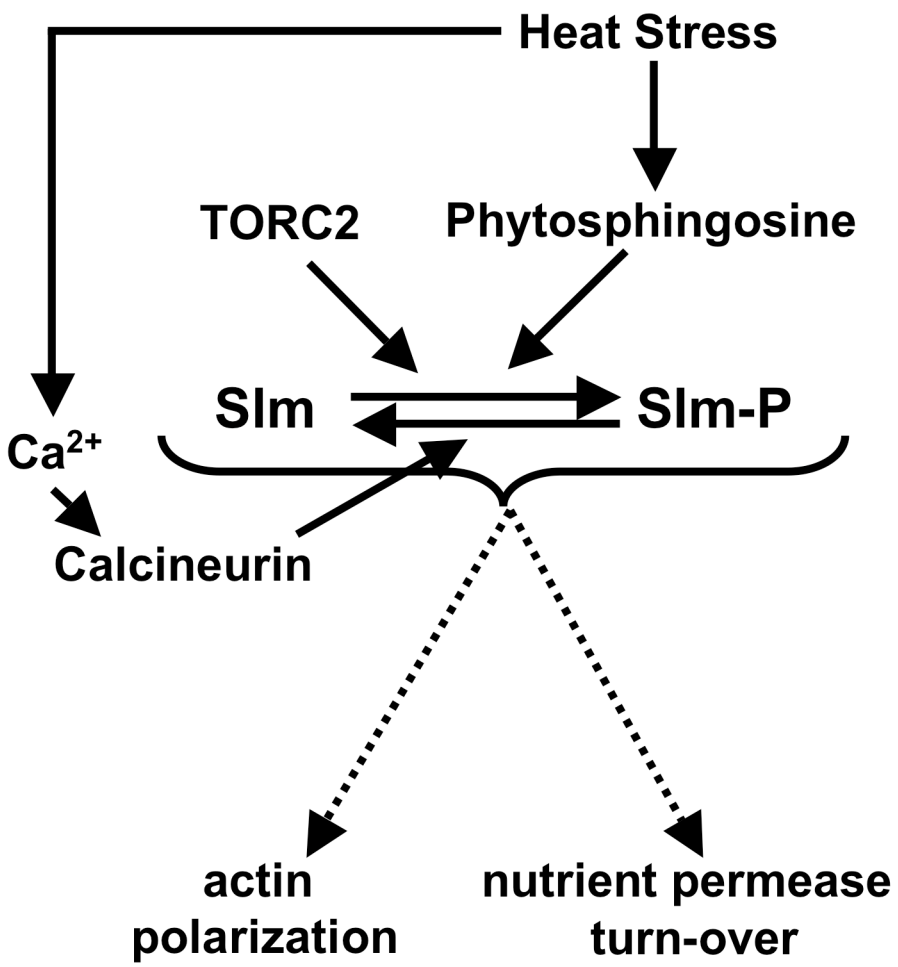
Heat Stress
TORC2
Phytosphingosine
Slm
Slm-P
Ca2+
Calcineurin
actin
polarization
nutrient permease
turn-over

Figure 11